Algal Research 40 (2019) 101492

Contents lists available at ScienceDirect

Algal Research

journal homepage: www.elsevier.com/locate/algal

Naked *Chrysochromulina* (Haptophyta) isolates from lake and river ecosystems: An electron microscopic comparison including new observations on the type species of this taxon

Chloe R. Deodato[a,1], Steven B. Barlow[b,1], Blake T. Hovde[c], Rose Ann Cattolico[a,*]

[a] Department of Biology, University of Washington, Box 351800, Seattle, WA, USA
[b] Department of Biology, San Diego State University, 5500 Campanile Drive MC-4614, San Diego, CA, USA
[c] Los Alamos National Laboratory, Bioscience Division, Los Alamos, NM, USA

ARTICLE INFO

Keywords:
Chrysochromulina
Freshwater
Scale-less
Electron microscopy
Morphology
Cryptic species complexes

ABSTRACT

Background: Chrysochromulina (Haptophyta) species are recognized as seminal contributors to marine and freshwater ecosystem function. Historically, scale vestiture is used to augment taxonomic identification of these algae, and a large literature exists concerning the morphology of many scale-covered representatives. Scale-less freshwater isolates present a new challenge. Details concerning the microanatomy of naked cells remain essentially unreported. Insight into morphological similarities/differences between scaled and naked cells provides information on the evolution of the taxon, especially as discussions defining cryptic species complexes become more germane. Using light, scanning, and transmission microscopy, we present an analysis of the cellular structure for three *Chrysochromulina* freshwater isolates.

Results: Chrysochromulina tobinii Cattolico, *Chrysochromulina parva* Lackey and *Chrysochromulina*$_{AND}$ cells are approximately 5 μm wide, saddle-shaped to globose, and devoid of scales. A lipid body is nestled close to each of two chloroplasts and numerous mitochondria. Plastoglobuli are frequently associated with thylakoidal membranes that encircle an internal pyrenoid. The Golgi apparatus has large, club-shaped cisternae. The haptonema consists of 9 microtubules within the cytoplasm, but 6 or 7 microtubules in the external portion. A rootlet system anchors the two flagella that are sub-apically inserted adjacent to the haptonema. The flagellar complex is anchored in the cytoplasm by a flat ribbon of microtubules and microtubular rootlets associated with each basal body. Fibrous rootlets, several of which are cross-banded, interconnect the two flagellar basal bodies and haptonema.

Conclusion: Three freshwater, scale-less *Chrysochromulina* isolates are almost indistinguishable in ultrastructure, even though extensive genome sequencing studies verify their distinctiveness. These freshwater representatives certainly comprise members of a cryptic species complex. Extensive morphological similarity also occurs between freshwater and scaled marine isolates. Importantly, this report addresses the misidentification of *Chrysochromulina tobinii* Cattolico as *Chrysochromulina parva* Lackey and clarifies a complex literature regarding the morphological description of the type species for this algal clade.

1. Introduction

Haptophytes represent an ancient and complex assemblage of algae whose evolutionary ascendance most likely took place approximately 1000 million years ago [1]. Accelerated awareness of the central role haptophytes play in the maintenance of global ecology [2–6] has promoted a continued re-assessment of the phylogeny of this algal taxon [7–9]. This awareness has also fostered new studies into the metabolic programs (e.g., lipid, toxin, DMS production) that enable the understanding of haptophyte contribution to aquatic biology and potentiate their commercial application [10–13].

Two classes of haptophytes are recognized – the Pavolvophycidae (4

Abbreviations: NCMA, Provasoli-Guillard National Center for Marine Algae and Microbiota; NIES, National Institute for Environmental Studies; SEM, Scanning electron microscopy; TEM, Transmission electron microscopy; BODIPY 505/515, 4,4-Difluoro-1,3,5,7-Tetramethyl-4-Bora-3a,4a-Diaza-s-Indacene

* Corresponding author.
E-mail addresses: chloed@uw.edu (C.R. Deodato), sbarlow@sdsu.edu (S.B. Barlow), hovdebt@lanl.gov (B.T. Hovde), racat@uw.edu (R.A. Cattolico).
[1] Co-first author.

https://doi.org/10.1016/j.algal.2019.101492
Received 7 November 2018; Received in revised form 26 March 2019; Accepted 3 April 2019
Available online 16 April 2019
2211-9264/ © 2019 The Authors. Published by Elsevier B.V. This is an open access article under the CC BY-NC-ND license (http://creativecommons.org/licenses/BY-NC-ND/4.0/).

orders) and Prymnesiophycidae (6 orders) [14]. Biodiversity within this algal taxon is well recognized [14–16], and morphological variability is extensive. Motile unicellular representatives can be spherical, bell, conical, or saddle-like in shape, and heteromorphic, diplontic life cycles are observed for some species [17]. Frequently, haptophyte microanatomy is associated with two specific cellular characteristics: (a.) the presence of a flagellar-like haptonema – a specialized appendage (vestigial in some representatives) that is posited to augment the recovery of food particles [18], and (b.) scale embellishment on the cell – a feature which often has taxonomic value. Architecturally, scales may be of simple, delicate configuration (e.g., patterned plates) or be of complex, multi-dimensional construct (e.g., coccoliths). More than one scale type may be found on a cell. Scale composition may be organic, or mineralized with silica or calcium carbonate [19]. Notably, haptophyte representatives having solely an extracellular mucilagenous coating have also been described [20,21].

Among haptophytes, *Chrysochromulina* (Prymnesiophyceae) ranks as one of the most prevalent genera. Representatives of this taxon are abundantly found in oceanic microplankton profiles [22–24] and can also reach high cell densities in lake ecosystems [3,5,25]. *Chrysochromulina* is truly a cosmopolitan organism. James Lackey first described the genus *Chrysochromulina* in 1938 [26] while analyzing a water sample from the Big Walnut Creek tributary of the Scioto River (Ohio, USA). The description of this alga, based on light microscopic observation, was of a 3–5 × 2–3 μm cell having two chromophores and three flagella – one of which was 5 to 8 times as long as the cell. No description of extracellular scale embellishment was noted. *Chrysochromulina parva* Lackey is considered to be the type species. Many new *Chrysochromulina* species, especially marine, were found beginning in the 1950's when electron microscopes became available (e.g., [27,28]). All species reported had scales. When examined by electron microscopy, a freshwater isolate (designated *Chrysochromulina parva* Lackey [29]), collected from Lake Windermere (England) was found to have delicate scales, as were isolates collected from additional freshwater locales (Table 1). Contemporary thought was that scales were so ephemeral in some *Chrysochromulina* isolates, that investigators did not see them, especially since most analyses used light microscopy [26], or that scales were actually lost during culture curation (Andersen pers. comm.). However, as early as 1985, scale-less *Chrysochromulina* isolates were also found in Canadian lakes [30] and more recently, in geographically dispersed locations (Table 1: see discussion below). Over time, the genus *Chrysochromulina*, which presently comprises approximately 60 species [14], was subdivided into additional genera [7]. Among these, three additional freshwater *Chrysochromulina* representatives were described: *C. breviturrita* [31], *C. laurentiana* [32], and *C. inornamenta* [33]. All have scales.

The goal of this study is to compare the morphology of three freshwater *Chrysochromulina* isolates: *Chrysochromulina tobinii* Cattolico [34], an isolate recovered from a Colorado lake, USA (identified as *Chrysochromulina parva* Lackey when it was submitted to the National Center for Marine Algae and Microbiota: strain CCMP291); *Chrysochromulina parva* Lackey, the "type species" re-isolated from Big Walnut Creek, Ohio USA (University of Washington: strain UW 1161); and an unnamed *Chrysochromulina* species (*Chrysochromulina*$_{AND}$) obtained from the Fox River (Illinois, USA).

Until this study, no one had re-isolated the *Chrysochromulina* "type species" (*Chrysochromulina parva* Lackey) from Big Walnut Creek, the type locality for the species since it was originally described in 1939. Revisiting the morphology of this recovered organism is especially important given the long-term controversy concerning the scale morphology of the type species, and the fact that new genomic data strongly support the observation that the *Chrysochromulina tobinii* Cattolico (CCMP291) and *Chrysochromulina parva* Lackey (UW 1161) isolates differ genetically [34].

2. Results and discussion

Micro-anatomical descriptions are described for the three freshwater *Chrysochromulina* isolates as: (a.) a detailed cellular analysis of *Chrysochromulina tobinii*, followed by (b.) corroborative morphological observations for *Chrysochromulina parva* and *Chrysochromulina*$_{AND}$. A discussion of scale vestiture and compilation of freshwater *Chrysochromulina* representatives is also presented.

2.1. I. Chrysochromulina tobinii Cattolico

Chrysochromulina tobinii Cattolico (CCMP291) is a halo-tolerant alga, growing robustly in low salinity (e.g., 8 mM NaCl) cultures, but able to survive higher salt concentrations (e.g., 32 mM; Fig. S1). Cells in the G1 phase of growth vary in shape and size, ranging from elongate (4–6 μm long by 3–4 μm wide), to globose (4–6 μm in diameter) by light microscopy. The organism is biflagellated, with equal or slightly subequal flagella, and has a coiling haptonema that is approximately 6–9 body lengths in size (Fig. 1A). The flagella and haptonema of elongated cells are inserted sub-apically near the anterior end of the organism (Fig. 1B, C) within a groove that runs the length of the organism. The presence of this groove leads to the description of many cells in this genus as being "saddle-shaped" (e.g., [48]). Several different swimming behaviors have been observed for this alga. With the haptonema fully extended, cells can move slowly through the water, either with or without helical rotation. While moving, the haptonema can assume different orientations relative to the cell body. When extended, the haptonema can be directed in front or trail behind the cell body (Fig. 1A). Alternatively, when coiled, the haptonema lies adjacent to the side of the cell (Fig. 1C). In either case, the two flagella are extended out the sides of the cell. Cells have been observed to suddenly start spinning around their axes, then very rapidly swim away. This swimming behavior is so rapid that determination of haptonema and flagella orientation is not possible. *Chrysochromulina tobinii* Cattolico shares many ultrastructural similarities to marine saddle-shaped *Chrysochromulina* species described in the literature (e.g., [48–51]) with a singular difference. The organism is naked, lacking scales on the cell surface, in the Golgi apparatus, or within intracellular vesicles. Ultrastructural details are presented below.

2.1.1. Nucleus

The nucleus is nestled between the two lateral chloroplasts, at the posterior end of the cell (Fig. 1D). Diffuse euchromatin and prominent patches of condensed heterochromatin are often observed near the nuclear periphery. A large, centrally located nucleolus that lacks substructure is consistently seen. Preliminary data show an estimated 22 chromosomes (Brewer, Deodato, and Cattolico, unpub.).

2.1.2. Chloroplasts

Each cell in the G1 phase of growth contains 2 peripheral chloroplasts that are flattened against the plasma membrane (Fig. 1D). As with other chloroplast-containing members of the Haptophyta [52], the outermost chloroplast membrane is continuous with the outer membrane of the nuclear envelope (Fig. 1E). The thylakoids, which can run the length of the organelle, are organized in layers of three (Fig. 1E). Neither girdle lamellae nor eyespots are present. The central portion of the chloroplast typically contains a large, immersed pyrenoid. Often visible within the pyrenoid matrix is a tubular structure parallel to the thylakoids (Fig. 1F). The true nature of this tube is somewhat uncertain, possibly representing a thylakoidal remnant. Similar pyrenoidal tubes have been observed in *Chrysochromulina apheles*, *Chrysochromulina bergenensis*, and *Chrysochromulina mantoniae* [51]. Plastoglobuli are scattered throughout the chloroplast matrix (Fig. 2A, C).

Although interphase cells were predominantly analyzed for this study, dividing cells that contained three or more chloroplasts were observed. Dividing chloroplasts appear to have thylakoidal bands that

Table 1
Representative geographical distribution of fresh water *Chrysochromulina* isolates with observations on scale vestiture.

Chrysochromulina isolate: published identifier	Geographical origin[c]	Scale type	Reference
C. sp. Andersen Culture lost	Fox River, Illinois, USA	Absent	This work
C. parva Lackey Culture collection UW 1161	Big Walnut Creek tributary of the Scioto River, Ohio, USA	Absent	This work
C. parva Lackey Field sample (holotype)	Big Walnut creek tributary of the Scioto River, Ohio, USA	Absent	[26]
C. tobinii Cattolico[a] Culture collection CCMP291	Alpine lake, Colorado, USA	Absent	This work; [10,34,35]
C. sp. Field sample	Dowdy lake, Lake John, Rolland Moore Park pond, Larimer County and South Delaney Buttes lakes Jackson County, Colorado, USA	Absent	[36]
C. parva Lackey Field sample	Escondido Lake and Ezquerra pond, San Carlos de Barioche, Argentina	Absent	[37]
C. parva Lackey Field sample	Vets and Elk ponds; Lakeview Turnpike marshes; Neosho River, Kansas, USA	1 type: Spider web; rim appears slightly raised	[38]
C. parva Lackey Field sample	Tarns in the English Lake Region, UK	1 type: Circular to oval delicate plates; spider web pattern on one face, radiating ridges on the opposite face	[29]
C. parva Lackey Field sample	Sadashivangar Tank, Banglore, Suraj Kund, Haryana, India	1 type: Circular to oval delicate plates; spider web pattern on one face, radiating ridges on the opposite face	[39]
C. parva Lackey Field sample	Brandenberg, Germany	1 type: Delicate, roundish scales of polysaccharide seen only by electron microscopy	[40]
Uncultured haptophyte[b]	Lake Stechlin, Germany	Microscopic analysis verifies *Chrysochromulina parva* abundance but with no morphological detail; Molecular data	[41]
*C. parva** Field sample	Freshwater ecosystems in Chevereuse, Tour, Vallees, Perray, Pourras Bourget, Annecy, France	Molecular data only	[5]
*C. parva**	Pyrenean mountain lakes, between Spain and France (227 sampled)	Molecular data only	[42]
Uncultured eukaryote[b]	Lake Ciso, Girona, Spain	Molecular data only	AJ862446
Uncultured eukaryote[b]	East Tibetan Plateau, freshwater High Lake 2, Quinghai, China	Molecular data only	[43]
C. parva Lackey* Field sample	Lake Tahiu, China	Molecular data only	[44]
C. parva Lackey* Culture collection NIES-562	Ibaraki, Japan	Molecular data only	[34]
*C. parva**	Ward Hunt lake, Canadian Artic	Molecular data only	[45]
C. breviturrita Field sample	Shield Lakes, Ontario, Canada	2 types: Complex outer spine containing scales with base plate; oval plate scales structured differently on upper and lower face	[14,31,32,46]
C. inornamenta Field sample	Lake Booker, Florida, USA	Oval scales with rim; no sculpturing	[14,33]
C. laurentiana Field sample	Experimental Lakes area L223, Ontario, Canada	Oval to diamond shaped scale with raised rim; sculptured or criss cross pattern on distal but not proximal face	[32]

[a] The isolate CCMP291 has now been shown by whole genome analysis to be *C. tobinii* Cattolico and not *C. parva* Lackey [34].

* Molecular studies often use the 18S r DNA sequence (accession number AM491019 [5]) designated "*Chrysochromulina parva*" (i.e., CCMP291) as the reference sequence for phylogenetic studies.

- Comparison of the AM491019 probe vs *C. parva* UW 1161 (redefined in our study) reveals three nucleotide differences exist between the two: 1 gap (position 181) and 2 single nucleotide changes-alterations are at position 561 (T to G) and at position 589 (G to C.).
- Use of the UW 1161 18S sequence (the type species) for further phylogenetic studies is encouraged.

[b] High sequence similarity to *C. parva* AM491019.

[c] Although *Chrysochromulina* has been reported to occur in Lake Baikal, Russia [47], re-examination of data suggests that further studies are necessary to verify this taxonomic assignment.

are positioned ~45° relative to one another (Fig. 2A). Recent genome sequence analysis of *Chrysochromulina tobinii* Cattolico (as well as *Chrysochromulina parva* Lackey) demonstrates conservation and duplication of the *fts*Z genes – one of which is novel to haptophytes [34]. FtsZ proteins determine the location of the division ring within the plastid and help recruit additional division proteins [53–55]. Presently, little mechanistic information is available concerning plastokinesis [56] in 4-membrane enclosed chloroplasts.

2.1.3. Mitochondria

Mitochondria are delineated by two membranes, of which the innermost forms tubular cristae (Fig. 2B). Fluorescent labeling suggests the presence of 2 to 3 mitochondria per *Chrysochromulina tobinii* Cattolico cell, while serial sections reveal a complex, most likely tentaculate, morphology for this organelle (data not shown).

2.1.4. Lipid bodies

The G1 phase cell contains two prominent lipid bodies that each lie nestled into the concave inner surface at the anterior of the plastid. Lipid bodies appear electron-translucent to electron-dense in thin sections (Fig. 2C). These organelles predominantly serve as neutral lipid storage compartments for the cell, but may have additional function, such as a site for the storage and degradation of proteins [57,58]. At the light microscope level, lipid bodies were identified by their retention of BODIPY 505/515 dye (Fig. 2C insert), which accumulates in lipidic compartments via a diffusion-trap mechanism [59]. Mitochondria are regularly juxtaposed closely to the surface of this organelle (Fig. 2C). When *Chrysochromulina tobinii* Cattolico cultures are subject to a 12 h light:12 h dark photoperiod (12 L:12D), lipid body volume shifts, being largest and smallest at the end of the light and dark periods respectively (see [10]; [60] for discussion).

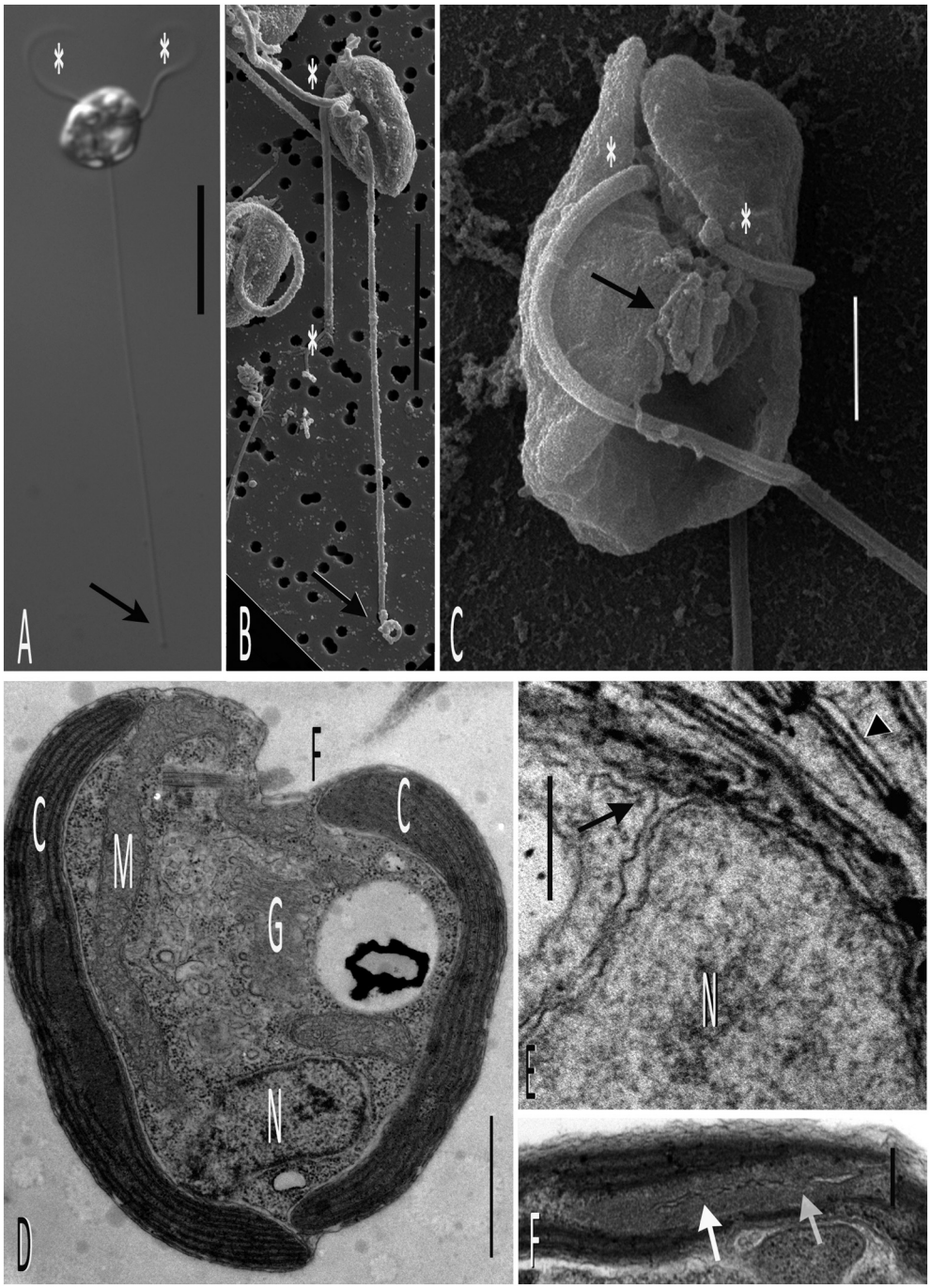

Fig. 1. Light, SEM and TEM observations of *Chrysochromulina tobinii* Cattolico.
A) Globose biflagellate cell, with extended haptonema (arrow) ~7 times the length of the cell and two flagella (asterisks). Nomarski optics scale bar = 10 μm.
B) Saddle-shaped cell, with longitudinal groove, extended haptonema (with coiled tip, arrow, and coils at the insertion point) and two flagella (asterisks). SEM scale bar = 5 μm.
C) Saddle-shaped cell, with longitudinal groove containing fully coiled haptonema (arrow), and two flagella (asterisks). SEM scale bar = 1 μm.
D) Whole cell, with 2 parietal chloroplasts (C) and embedded pyrenoid (P), Golgi apparatus (G), posterior nucleus (N) with chromatin and nucleolus, and subapical insertion of flagella/haptonema within a groove in the cell (F). TEM scale bar = 1 μm.
E) Outer chloroplast and nuclear membranes are continuous (arrow), and thylakoids stacked in layers of three (arrowhead). TEM scale bar = 200 nm.
F) Embedded pyrenoid with penetrating tubule (arrows). TEM scale bar = 250 nm.

2.1.5. ER and Golgi

The Golgi apparatus consists of 10 to 20 stacked cisternae (Fig. 2D, E) adjacent to vesicles believed to be vacuolar in nature. The edges of the cisternae closest to the vacuole are flattened and tightly appressed compared to the opposite side of the cisternal stack which appears inflated, giving the cisternal cross-section a wedge-like configuration (Fig. 2E). This cisternal morphology has been observed in other *Chrysochromulina* species [51]. There is no evidence of any scale material in the Golgi cisternae, or in cellular vesicles (Fig. 2D, E). There are no external plates or scales on the outside of this naked cell (Figs. 1D, 2A, C).

2.1.6. Flagella and haptonema

The haptonema and flagellar apparatus are closely associated (Fig. 3A). The haptonema of *Chrysochromulina tobinii* Cattolico consists of 6–9 microtubules inside the cell, but 6 microtubules in cross-section when viewed outside the cell body (Fig. 3B). In many cases, fine electron-dense connections can be seen between adjacent tubules. Also present along the length of the haptonema is a vesicular compartment (Fig. 3A, B) that is an extension of the cytoplasmic endoplasmic reticulum [61,62].

The basal bodies of the two *Chrysochromulina tobinii* Cattolico flagella are oriented at approximately 90° relative to each other. Using the rootlet nomenclature of Eikrem and Moestrup [49], basal body 2 (BB2) terminates midway along the length of basal body 1 (BB1) (Fig. 3A). Fibrillar electron-dense material connects the terminus of BB2 to the side of BB1. Each flagellum exhibits a pair of basal plates distal to the basal body. These plates occur as electron-dense lines in longitudinal slices of the flagella (Fig. 3A) and appear as intra-tubular electron-dense connections when viewed in flagellar cross section. The distal flagellar

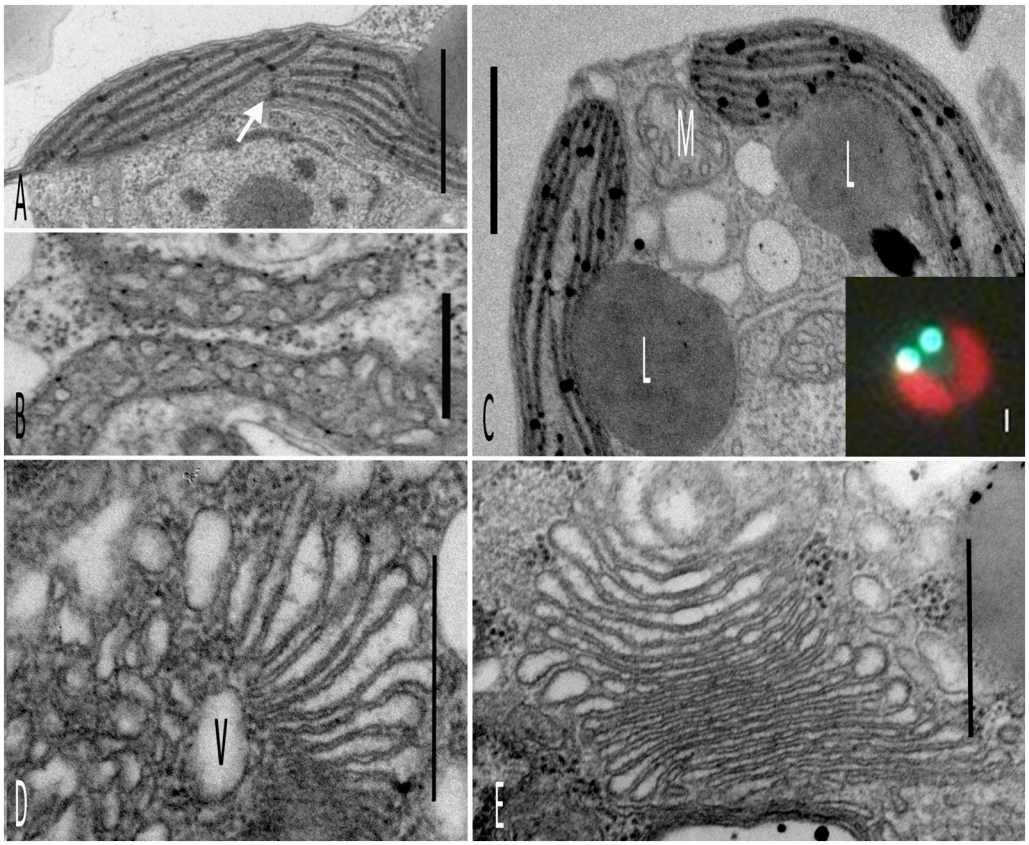

Fig. 2. *Chrysochromulina tobinii* Cattolico chloroplast, mitochondria, lipid bodies, and Golgi apparatus.
A) Dividing chloroplast, with daughter thylakoids oriented approximately 45° to each other (arrow). TEM scale bar = 1 μm.
B) Mitochondrial profiles with tubular cristae. TEM scale bar = 200 nm.
C) Lipid bodies (L) and associated mitochondria. TEM scale bar = 1 μm. Insert: Chloroplasts autofluoresce red, lipid bodies stained with BODIPY 505/515 dye [59] are aqua. Fluorescence microscopy scale bar = 1 μm.
D) Golgi apparatus, showing inflated wedge-shaped lamella, and adjacent presumptive vacuole (V). TEM scale bar = 500 nm.
E) Golgi apparatus, showing stacked cisternae. TEM scale bar = 500 nm. (For interpretation of the references to colour in this figure legend, the reader is referred to the web version of this article.)

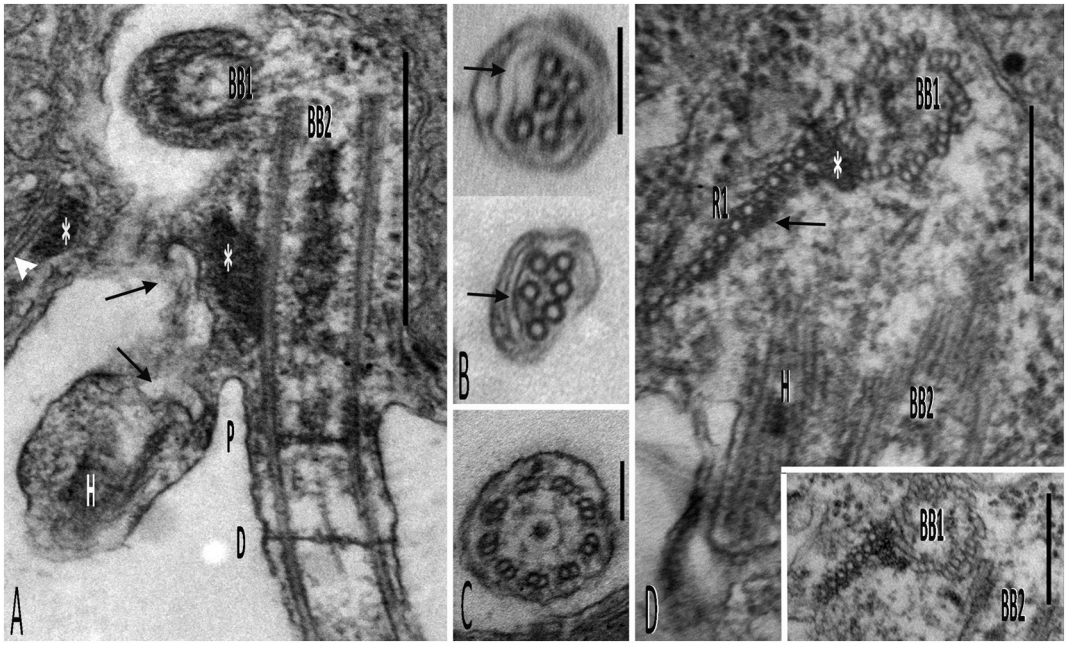

Fig. 3. *Chrysochromulina tobinii* Cattolico basal body and haptonema microtubule embelishment.
A) The two basal plates, proximal (P) and distal (D) are visible near Basal Body 2 (BB2). The haptonema (H) lies adjacent, and endoplasmic reticulum can be seen extending into it (arrows). Basal Body 1 (BB1) is seen perpendicular to BB2. Parts of the electron-dense Distal Fiber are visible (asterisks), extending between BB2 and the microtubule R1 rootlet (arrowhead). TEM scale bar = 500 nm.
B) Two different cross-sections of the haptonema reveal differing orientation of the 6 haptonemal microtubules, with electron-dense crosslinks and haptonemal endoplasmic reticulum (arrows). TEM scale bar = 100 nm.
C) Distal plate of basal body in cross-section. Electron-dense connections resemble a wagon wheel. TEM scale bar = 200 nm.
D) Rootlet R1, here composed of 13 microtubules, decorated along one side with electron-dense material (arrow), attaches to the side of BB1 via electron-dense plaque (asterisk). TEM, tilted 20°, scale bar = 300 nm. Insert: another section of the same R1 rootlet serial ribbon exhibits only 7 microtubules. The number of microtubules in the ribbon increases in number as the ribbon extends into cytoplasm. TEM, tilted 0°, scale bar = 300 nm.

plate resembles a wagon wheel whose electron-dense spokes radiate out to each of the flagellar doublets (Fig. 3C).

2.1.7. Microtubular rootlets

There are four microtubular rootlets, 2 sets per basal body. All appear to attach to the basal bodies via electron-dense pads. A flat ribbon of microtubules (R1) originates in an electron-dense layer located adjacent to BB1. Most commonly, the ribbon appears as 7–9 microtubules. However, it has been observed in some sequential sections (Fig. 3D) that the number of microtubules can increase distally from 7 to 9 at the proximal end of the ribbon of microtubules (Fig. 3D, D insert) to about 15. A similar increase in the number of R1 microtubules is seen in sequential cross-sections of *Chrysochromulina acantha* [63,64], but whether this change in microtubule number in *Chrysochromulina tobinii* Cattolico represents a common occurrence or an early stage in rootlet and basal body reproduction could not be determined. A portion of the R1 ribbon is always observed alongside the flattened side of a mitochondrion, as reported for other saddle-shaped *Chrysochromulina* species [51]. In some cells, the proximal portion of the R1 rootlet is covered with an electron-dense layer along the side of the ribbon facing away from the mitochondrion (Fig. 3D). Distally, the R1 ribbon of microtubules splits into two groups: a group of 4–5 tubules closest to BB1 splay apart and pass individually through the cytoplasm toward the adjacent chloroplast, and the remaining microtubules of the ribbon extend as a flattened ribbon alongside a mitochondrion toward the adjacent chloroplast. The second microtubular rootlet, R2, located on the opposite side of BB1 from the R1 ribbon, consists of 1–2 tubules that are very short and oriented parallel to BB2, and pass between two cross-banded fibers that connect BB2 and the haptonema (Fig. 4A, B). The second basal body, BB2, also exhibits two rootlets, R3 and R4 (Fig. 4A, B). R3 begins in an electron-dense mass located to the outside of BB2 and consists of 3 microtubules, usually arranged in a 2 over 1 orientation (Fig. 4C). As it extends between a chloroplast and the plasmalemma, the microtubule number may increase to a 4-in-line or a three-over-one orientation. The R4 rootlet, originating on the side of BB2 that faces the haptonema and BB1 and on the opposite side of BB2 as R3, consists of 2–3 microtubules (Fig. 4D). In *Chrysochromulina ahrengotii* [48] the single R4 rootlet extends into the cytoplasm and joins with the microtubules of the R3 rootlet. We could not determine if a similar merging of the R3 and R4 rootlets occurs in *Chrysochromulina tobinii* Cattolico.

2.1.8. Fibrillar rootlets

There are several fibrillar rootlets connecting the basal bodies and haptonema. A large fibrillar distal fiber (DF) extends between BB2 and the opposite R1 microtubular ribbon (Figs. 3A, 4A, B). No distinctive connections were observed at the junction between the distal fiber and the microtubular R1 ribbon. Associated with this distal fiber is a wide, banded fiber extending between BB2 and the haptonema (Fig. 4E). Narrow, elongate, cross-banded fibers also extend from either side of BB2 to the haptonema (Fig. 4B). In some cells, a single elongate, cross-banded fiber also appears to connect BB1 with the haptonema.

2.2. II. *Chrysochromulina parva* Lackey and *Chrysochromulina*$_{AND}$

To corroborate and extend the observations made for *Chrysochromulina tobinii* Cattolico preliminary SEM and TEM analysis of two additional freshwater isolates have been made.

Chrysochromulina parva Lackey was isolated in 2014 from Big Walnut Creek, Shadeville, Ohio at a site close to that in which the type species *Chrysochromulina parva* Lackey was initially found [26]. Whole genome sequence comparison shows *Chrysochromulina tobinii* Cattolico and *Chrysochromulina parva* Lackey to differ genetically. For example, almost 1000 single nucleotide polymorphisms occur between the mitochondrial coding regions of these two isolates [34]. A third *Chrysochromulina* isolate, *Chrysochromulina*$_{AND}$ was collected by Celia Lopez from the Fox River near McHenry, Illinois in 1981. The alga was isolated into culture, and at that time was fixed and embedded for TEM by Dr. Robert A. Andersen. The fixed organism was never examined in detail and the EM blocks remained in storage until our studies. Unfortunately, a living *Chrysochromulina*$_{AND}$ culture is no longer available, thus we were not able to generate genetic information for this isolate.

2.2.1. Comparative morphology of *Chrysochromulina parva* Lackey and *Chrysochromulina*$_{AND}$

Chrysochromulina parva Lackey is approximately 4–5 μm in size (Fig. 5A, B) when analyzed by light microscopy, with a longitudinal groove clearly visible by SEM (Fig. 5C). The haptonema appeared as much as thirteen times the body length, slightly longer than that observed for *Chrysochromulina tobinii* Cattolico. Because this organelle is very dynamic, and can exhibit coiling and uncoiling, the observed differences in maximum haptonemal length should not be considered as a definitive taxonomic character. Given that live cultures of *Chrysochromulina*$_{AND}$ are no longer available, analysis of *Chrysochromulina*$_{AND}$ size and shape could only be estimated from TEM sections. These observations suggest a cell size of about 5 μm and the presence of a groove (Fig. 7A). TEM analysis reveals that both *Chrysochromulina parva* Lackey and *Chrysochromulina*$_{AND}$ are naked cells. No scales are seen on the cell exterior (Figs. 5D, 7A) or in the internal vesicles or Golgi of either isolate (Figs. 5G, 7A, B, C).

A nucleus with its prominent nucleolus is located in the posterior of the cell between the two chloroplasts in both *Chrysochromulina parva* Lackey and *Chrysochromulina*$_{AND}$ (e.g., Fig. 5D). The two peripheral chloroplasts of both isolates (Figs. 5D, 7A) are each enclosed by a periplastidial membrane that is continuous with the outer nuclear membrane (e.g., Fig. 7D). Chloroplasts have an embedded pyrenoid (Figs. 5D, 7A) that is fenestrated by a single tubule (Figs. 5E, 7E). Multiple mitochondrial profiles, exhibiting tubular cristae, are visible in most sections (Figs. 5D, F, 7A).

Each *Chrysochromulina parva* Lackey and *Chrysochromulina*$_{AND}$ cell has two large lipid bodies as well as several large vesicles containing electron-opaque material (Figs. 5D, 7A). The Golgi apparatus of these two isolates contains multiple cisternae (e.g., Fig. 7B), some of which are wedge-shaped (Figs. 5G, 7C).

The flagella and haptonema of both *Chrysochromulina parva* Lackey and *Chrysochromulina*$_{AND}$ insert into a groove in the cell (Figs. 5C, 7A), although the details of this groove could not be easily ascertained from thin slices generated for *Chrysochromulina*$_{AND}$. It was not possible to determine the relative length of the *Chrysochromulina*$_{AND}$ haptonema from the sections produced in this study, but clearly a portion, if not all, of the haptonema can coil (Fig. 8A). In both *Chrysochromulina tobinii* Cattolico and *Chrysochromulina parva* Lackey, the haptonema has 6 microtubules in the portion of the organelle that extends from the cell body (Figs. 3B, 6B), whereas *Chrysochromulina*$_{AND}$ has 7 (Fig. 8B). It is important to note that the naked, freshwater *Chrysochromulina parva* Lackey we isolated from a site near the original *Chrysochromulina parva* Lackey discovery [26] has 6 microtubules in the external haptonema, when compared to the freshwater scale-covered *Chrysochromulina parva* described from the English Lake District [29] which has 7 microtubules in its external haptonema. Haptonema microtubular number varies among *Chrysochromulina* species, from 6 (*Chrysochromulina apheles*, *Chrysochromulina camella*, *Chrysochromulina companulifera*, *Chrysochromulina cymbium*, *Chrysochromulina strobius*, *Chrysochromulina throndsenii*) to 7 (*Chrysochromulina acantha*, *Chrysochromulina ephippium*, *Chrysochromulina scutellum*, *Chrysochromulina simplex*) in these saddle-shaped organisms [49]. Haptonemal endoplasmic reticulum (Figs. 3A, B, 6B) is commonly observed. While there is no molecular data available for the *Chrysochromulina*$_{AND}$ isolate, the difference in haptonemal microtubules clearly differentiates this morphologically-similar isolate from either *Chrysochromulina tobinii* Cattolico or *Chrysochromulina parva* Lackey.

In *Chrysochromulina parva* Lackey and *Chrysochromulina*$_{AND}$, two

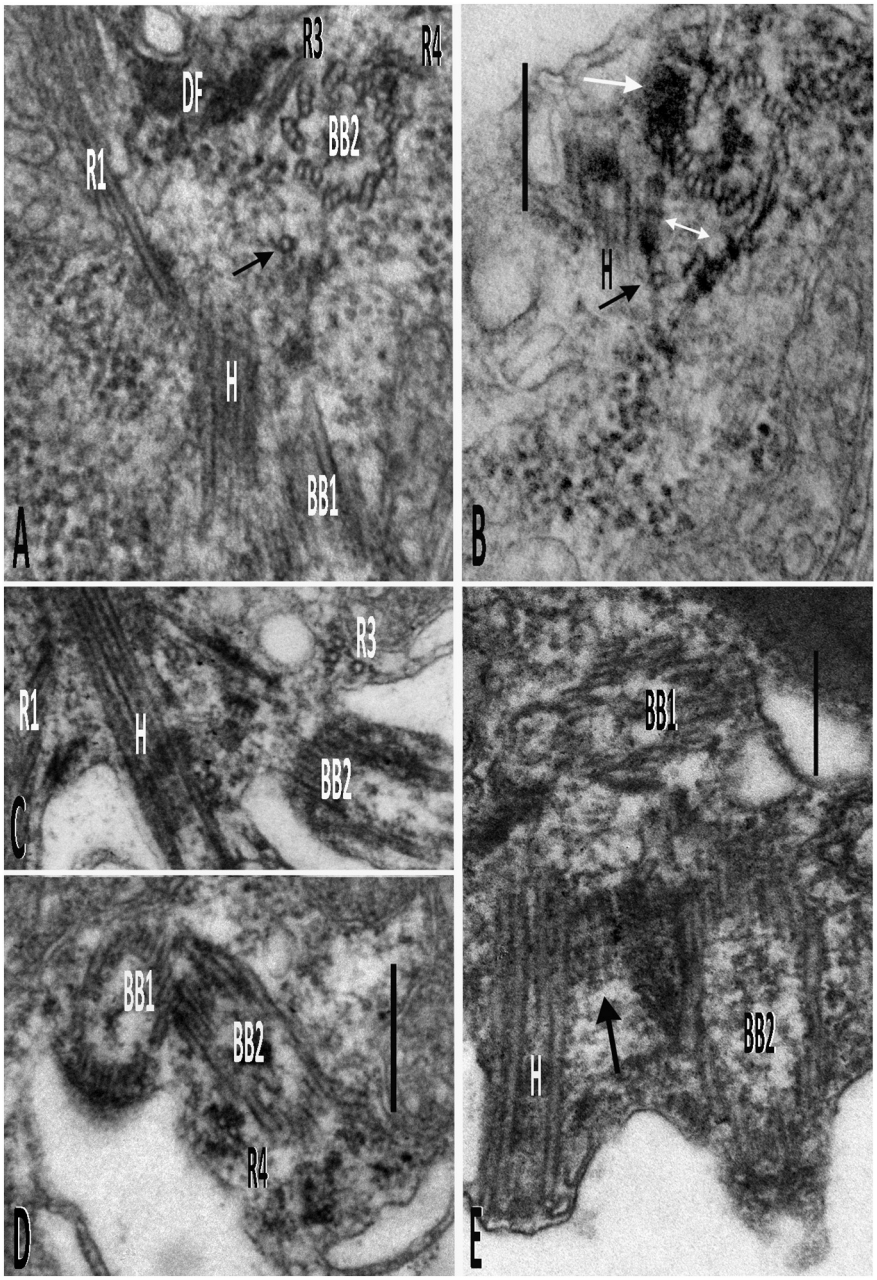

Fig. 4. *Chrysochromulina tobinii* Cattolico flagellar microtubule complement.
A) The Distal Fiber (DF) extends from BB2 toward the R1 microtubular ribbon. The oblique views of R3 and R4 microtubular rootlets are visible adjacent to the cross-section of BB2. Glancing oblique slice through the haptonema and BB1 show relative positions of these components. The single microtubule rootlet R2 is seen in cross-section (black arrow). TEM, tilted 36.6°, scale bar = 200 nm (in 6B).
B) An additional section through same rootlet serial shown in Fig. 6A. The attachment of the DF to BB2 is seen (white arrow), as well as two elongate cross-banded haptonemal fibers (double-ended arrow) extending from either side to BB2 toward the haptonema, seen in Fig. 6A. The single tubule of R2 is still visible (black arrow). TEM, tilted 36.6°, scale bar = 200 nm.
C) The R3 rootlet extending from the side of BB2 into the cytoplasm is seen here as a 2-over-1 configuration (R3). The electron-dense origination plaque is not visible in this section. TEM scale bar = 250 nm (in 6D).
D) Additional slice through the same rootlet serial as in Fig. 6C showing the electron-dense origin of 2 microtubules of rootlet R4 (R4). TEM scale bar = 250 nm.
E) A fibrous, cross-banded root (arrow) extends between BB2 and the haptonema (H). TEM scale bar = 200 nm.

basal bodies are oriented approximately ninety degrees relative to each other with BB2 terminating about the middle of BB1 (Fig. 8F, G). Both microtubular and fibrous rootlet systems are associated with the two flagellar basal bodies (BB1 and BB2) and the haptonema (H). The R1 rootlet consists of a flat ribbon of microtubules, varying in number but most commonly 9–12 in complement (Figs. 6C, 8E). The first microtubule of the ribbon is attached by electron-dense material to BB1 (Figs. 6C, 8F), and initially the tubules in the ribbon are oriented parallel to each other and to the long axis of BB1. This ribbon extends toward one of the chloroplasts alongside a mitochondrion (Fig. 8E–H). The 4–6 microtubules in the ribbon closest to BB1 spread apart as they extend into the cell cytoplasm (e.g., Fig. 8H). The rest of the microtubules in the ribbon remain as a flat sheet as they extend toward the adjacent chloroplast. A second rootlet (R2), also attached to BB1 by electron-dense material, is composed of 2 very short microtubules that extend toward BB2. On either side of BB2 are microtubular roots R3 and R4, each of which originate in an electron-dense plaque. Rootlet R3 consists of 4 microtubules arranged in either a 2–2 or 3–1 orientation where they originate at BB2, but seem to diminish to 3 microtubules as the rootlet extends under the plasmalemma alongside the chloroplast adjacent to BB2. The second rootlet, R4, originates alongside BB2 on the side of the basal body adjacent to the haptonema. The two microtubules in this rootlet are very short.

A distal fiber, without apparent banding, extends from the side of BB2 past the haptonema, ending adjacent to the flat ribbon of microtubules originating alongside BB1 (Figs. 6C, D, 8G, H). This fibrous root ends at the R1 microtubular rootlet, and in *Chrysochromulina*$_{AND}$ appears to attach to the microtubules of the R1 rootlet by fine electron-dense connections (Fig. 8H). Cross-banded fibrous roots extend from the sides of BB2 and attach to the side of the haptonema (Fig. 8F), while in *Chrysochromulina*$_{AND}$ an elongate crossbanded haptonemal fiber connects BB1 to the haptonema (Fig. 8G).

Each of the two flagella in both *Chrysochromulina parva* Lackey and *Chrysochromulina*$_{AND}$ has a single basal body at its proximal end. Similar to *Chrysochromulina tobinii* Cattolico, the transition region between flagellum and basal body is characterized by the presence of two

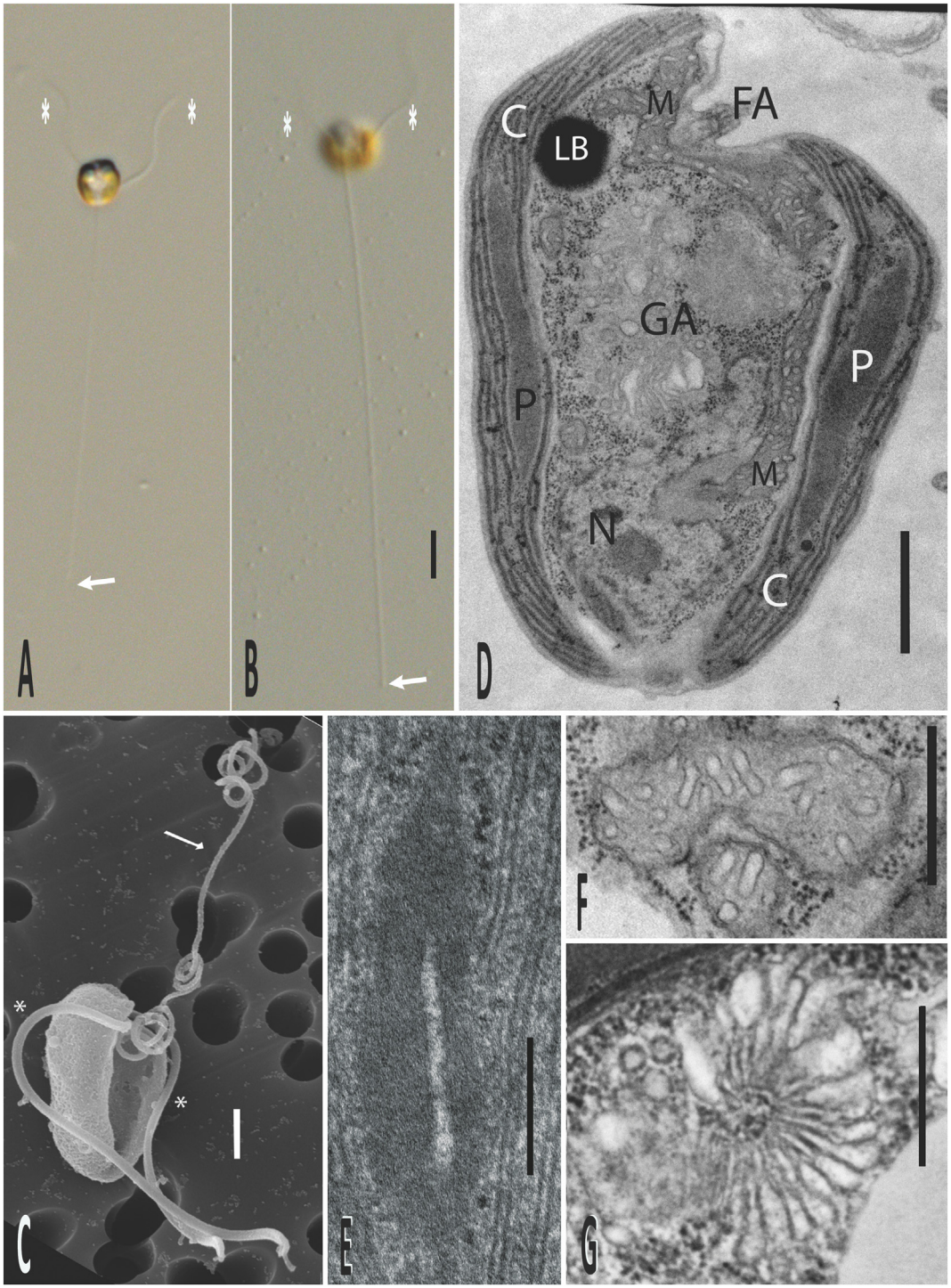

Fig. 5. *Chrysochromulina parva* Lackey light, SEM, and TEM analysis.
A, B) Whole cell LM images (Nomarski optics) *Chrysochromulina parva* Lackey. A) Longitudinal view of a globose-shaped cell with 2 flagella (asterisks) and extended haptonema ~ 6 times the length of the cell. The lipid body associated with each chloroplast appears as a bright dot. B) The intersection of the two flagella and haptonema in a groove in the cell is imaged, and the extended haptonema is ~10× the cell body length. Scale bar = 5 μm.
C) SEM of cell showing the longitudinal groove with antapical insertion of the 2 flagella (asterisks) and the partially coiled haptonema (arrow). Scale bar = 1 μm.
D) Whole cell TEM image showing the 2 lateral chloroplasts with embedded pyrenoid (P), mitochondria (M), Golgi apparatus (GA), and flagellar apparatus inserted into a groove in the cell. Scale bar = 1 μm.
E) Embedded pyrenoid with tubular inclusion. Scale bar = 200 nm.
F) Mitochondria with tubular cristae. Scale bar = 500 nm.
G) Golgi apparatus with wedge-shaped cisternae. Scale bar = 500 nm.

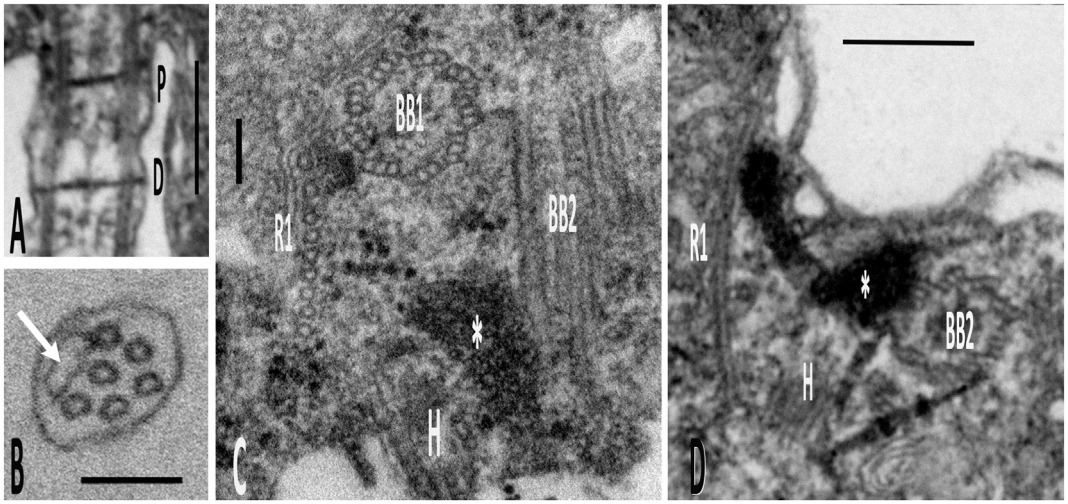

Fig. 6. *Chrysochromulina parva* Lackey haptonema and flagellar microanatomy.
A) Flagellar proximal (P) and distal (D) plates. Scale bar = 250 nm.
B) Haptonema cross-section showing 6 microtubules and E.R. compartment (arrow). Scale bar = 100 nm.
C) Flat microtubular ribbon of 9 microtubules attached by e-dense pad to BB1, Distal Fiber (asterisk) extending from BB2 past the haptonema (H) toward the flat microtubular ribbon. Scale bar = 100 nm.
D) Elongate cross-banded roots extending from BB2 to the haptonema (H) and Distal Fiber (asterisk) from BB2 to the flat microtubular ribbon, seen in longitudinal view. Scale bar = 100 nm.

electron-dense plates (Figs. 6A, 8C). In cross-section, the distal plate consists of electron-opaque connectors between doublets, in the shape of a wagon wheel, as well as a central plug (Fig. 8D), whereas the proximal plate only consists of microtubule doublets arranged in an interconnected circle and a central plug (Fig. 8E).

2.3. Phylogeny

Striking in the microanatomy assessment of three freshwater *Chrysochromulina* isolates is the saddle-shaped morphology of the cell – an architecture Estep [65] suggests maximizes the area available for auxotrophic chemical receptors. Also noteworthy is the complete lack of scales either on the surface of the organism or within intracellular vesicles. Electron microscopic observations made by our laboratory using cultures originally obtained in Colorado; one generated from Big Walnut Creek (Ohio); a sample from the Fox River (Illinois); as well as high-resolution analysis of *Chrysochromulina* by other investigators (e.g., the analysis of viral infected *Chrysochromulina tobinii* cells [35]) reveal a scale-less cell morphology. The fact that the cultures in which *Chrysochromulina* retains a naked morphology have been obtained from several geographic locales; curated by different investigators; maintained in dissimilar growth media (e.g., DY-V, RAC-5, or lake water plus Alga-Gro [66]); subjected to several temperatures (15 to 20 °C) or photoperiods (12 h light:12 h dark; 16 h light:8 h dark) during laboratory maintenance, and then subject to various EM preparation procedures, argues that the scale-less morphology is not an artifact of culture or of EM preparation [17].

So why do some *Chrysochromulina* isolates lack scales? As noted above, documented haplo-diplo life cycles that are correlated with distinct cellular morphotypes have been reported for several haptophyte taxa [17,67]. Mostly, changes in ploidy level are reflected by a modification in cellular scale type. For example, when *Chrysochromulina palpebralis* cells shift from tetraploid to haploid, cells are embellished with 3 and 2 scale types, respectively [16]. *Chrysochromulina*

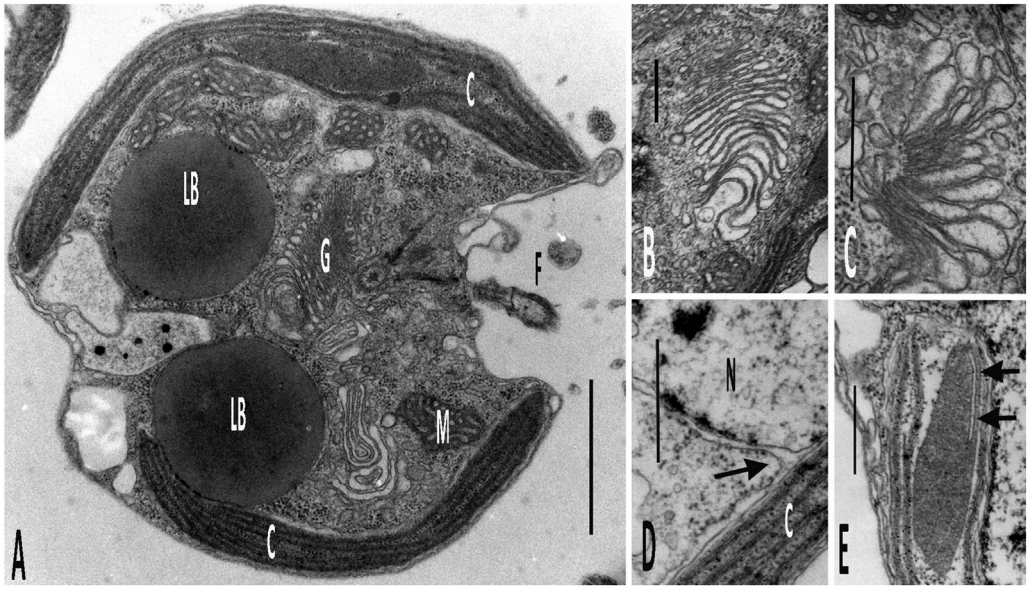

Fig. 7. *Chrysochromulina*$_{AND}$ microanatomy.
A) *Chrysochromulina*$_{AND}$ whole cell, with anterior lipid bodies (LB), 2 parietal chloroplasts (C), embedded pyrenoid (P), Golgi apparatus (G), and subapical insertion of flagella/haptonema (F) in a groove in the cell. TEM scale bar = 1 µm.
B) Golgi apparatus, showing stacked cisternae. TEM scale bar = 500 nm.
C) Golgi apparatus, showing wedge-shaped cisternae. TEM scale bar = 500 nm.
D) Continuity between outermost chloroplast membrane and the outer nuclear envelope (arrow), and heterochromatin and nucleolus in the nucleus (N). TEM scale bar = 500 nm
E) Embedded pyrenoid with penetrating tubule (arrow). TEM scale bar = 500 nm.

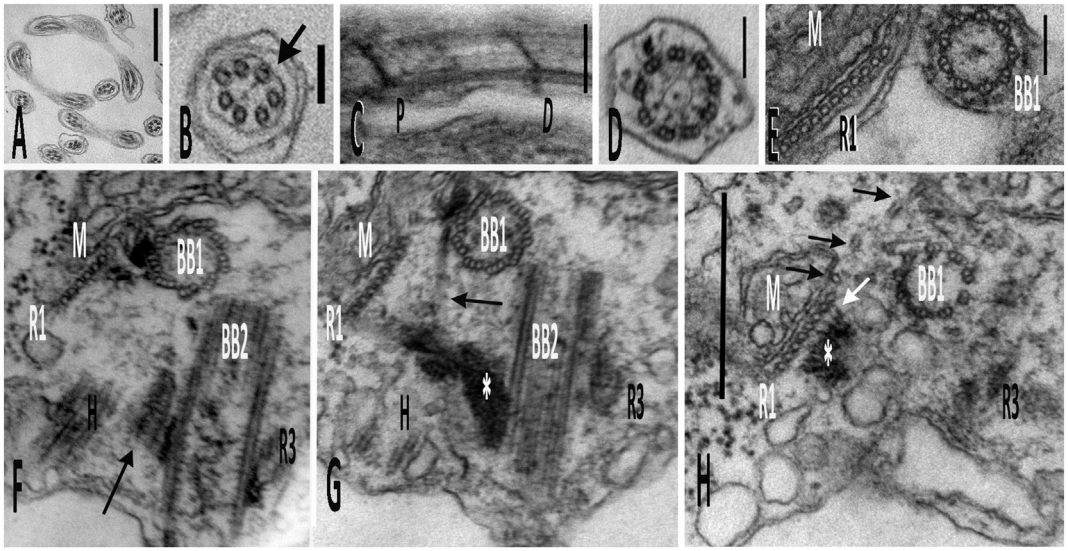

Fig. 8. *Chrysochromulina*$_{AND}$ haptonema and flagellar structural analysis.
A) Coiled haptonema seen in section. TEM scale bar = 500 nm.
B) The 7 haptonemal microtubules and crosslinks are visible in cross-section and haptonemal endoplasmic reticulum is indicated (arrow). TEM scale bar = 100 nm.
C) The two basal plates, proximal (P) and distal (D) are visible in longitudinal section. TEM scale bar = 100 nm.
D) The distal plate of the flagellum contains a wagon-wheel shaped assemblage of electron-dense interconnections. TEM scale bar = 125 nm.
E) Cross-section of the proximal plate of BB1, showing interconnections of microtubular doublets. Rootlet R1, with 11 microtubules, is also seen in cross-section adjacent to a mitochrondrion (M). TEM scale bar = 125 nm.
F–H) These three images are from a serial series, sequence #s 13(8F), 15(8G), and 17(8H). TEM Scalebar = 250 nm (in 8H). F) The R1 rootlet (R1) is aligned alongside a mitochondrion (M). G) An elongate cross-banded fibrous rootlet (arrow) extends from BB1 toward the haptonema (H), seen here in glancing section. The electron-dense Distal Fiber (asterisk) extends from BB2 to the R1 ribbon of microtubules adjacent to a mitochondrion. Rootlet R3 is seen in longitudinal view adjacent to BB2. H) The ribbon of microtubules in rootlet R1 are attached via electron-dense fibers (white arrow) to the distal fiber (asterisk). Some microtubules of the R1 microtubular ribbon are seen more longitudinally oriented as they separate from the rest of the cross-sectioned R1 ribbon (black arrows). Microtubules of the R1 rootlet (black arrows) separate and turn away from the ribbon and each other as they extend into the cell cytoplasm.

polylepis reflects ploidy state by transitioning between two morphotypes that differ both in cell size and in scale vestiture [67]. A ploidy-morphotype conversion is not seen in all *Chrysochromulina* taxa. Most *Chrysochromulina* species are haploid. Documentation of a full meiotic and recombination gene complement in *Chrysochromulina tobinii* Cattolico and *Chrysochromulina parva* Lackey shows sexual reproduction in these haploid isolates appears to be fully potentiated [10,34]. Interestingly, a hypothesis posited by Niklas and colleagues [68] argues that meiosis evolved before sexual reproduction as a method for rectifying spontaneous whole genome duplication (aneuploidy). If still in effect, this mechanism could also explain the presence of genes for recombination and repair.

Whether scale-less marine forms of *Chrysochromulina* exist remains an open question. Certainly, both scaled and naked isolates of

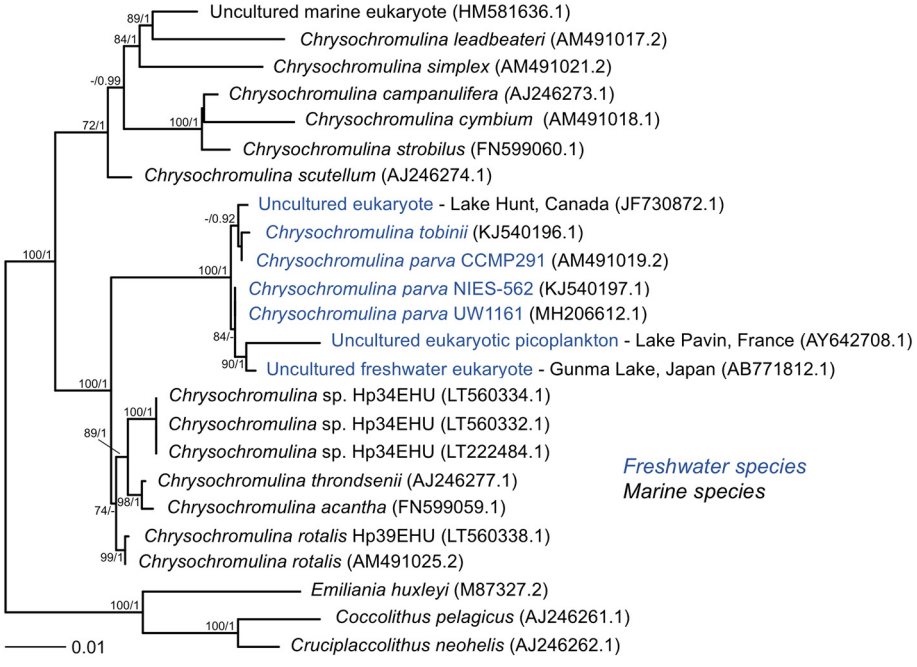

Fig. 9. Phylogenetic analysis of selected *Chrysochromulina* 18S small ribosomal subunit sequences. *Chrysochromulina tobinii* Cattolico 18S rRNA sequence probe that was used in the construct of this phylogeny differs from the published 18S rRNA CCMP291 NCMA sequence (Table S2). We find a guanine at position 181 whereas GenBank: AM491019.2 has a deletion at this site [10]. Independent Bayesian and maximum likelihood (ML) analyses estimated the same tree topology. Numbers indicate ML bootstrap values above 70 and Bayesian posterior probabilities above 0.80 respectively. Branch lengths shown are from the ML estimation. Genbank accession numbers for sequences are included in parentheses.

Chrysochromulina are known to be present in freshwater ecosystems that range from small ponds to rivers. Given the frequency of freshwater lineages arising within the haptophyte phylogenetic tree [3,5,69], it will be interesting to know if genes critical to scale formation are eliminated (provide vulnerable targets?) as an ancillary consequence of a marine to freshwater transition. Unfortunately, the fragile and delicate nature of some *Chrysochromulina* scale types [29] can make determination of their presence illusive. Although our efforts to identify molecular markers for scale generation have yet to be successful, we certainly know that the metabolome of freshwater and marine *Chrysochromulina* are differently impacted. For example, betaine, a key determinant in the maintenance of osmotic balance, is produced by osmotolerant *Chrysochromulina tobinii* Cattolico at 10 times the level of a marine *Chrysochromulina* isolate [12].

The occurrence of scale-less, freshwater *Chrysochromulina* strains has only been verified by micro-anatomical analysis for isolates found in North and South America. Although molecular studies strongly support fact that *Chrysochromulina*-related algae are present in many European and Asian freshwater ecosystems (Table 1), whether these isolates are scale-less, awaits further morphological study. The fact that micro-anatomical similarities between the North American *Chrysochromulina tobinii* Cattolico and *Chrysochromulina parva* Lackey fail to reflect their extensive genetic differences [34] argues that scale-less representatives (regardless of geographic origin) most likely will form a cryptic species complex. Such data also suggests that strong stabilizing selection may be in play [34,70].

Assessment of the relationship among *Chrysochromulina* species is presented in Fig. 9. A paucity of genomic data for this clade dictates that 18S ribosomal gene sequences are used in this analysis. *Chrysochromulina parva* Lackey and *Chrysochromulina tobinii* Cattolico show as much difference from one another as recognized closely related *Chrysochromulina* species within this clade (e.g., *Chrysochromulina acantha* and *Chrysochromulina throndsenii*). Also evident are significant phylogenetic differences among freshwater isolates.

2.4. Chrysochromulina "type species"

As noted in the Introduction, there has been a long-standing confusion in the literature on whether scales are present or absent on *Chrysochromulina parva* Lackey (e.g., Table 1, [26,29,38]). The re-isolation of *Chrysochromulina* from near the 1938 study site, and re-examination of the morphology of this organism that is presented here, argues that naked *Chrysochromulina parva* Lackey (UW 1161) represents the holotype for the taxon (See [34] for discussion). This conclusion is further supported by genome sequencing comparisons of *Chrysochromulina parva* Lackey (UW 1161) and *Chrysochromulina tobinii* Cattolico (CCMP291), showing them to differ [34]. *Chrysochromulina tobinii* Cattolico, *Chrysochromulina parva* Lackey, and *Chrysochromulina*$_{AND}$ share many morphological features. However, a difference in haptonemal microtubular number for *Chrysochromulina tobiniii* (6), *Chrysochromulina parva* (6), with that of *Chrysochromulina*$_{AND}$ (7), suggests *Chrysochromulina*$_{AND}$ remains an undescribed species. Regrettably, *Chrysochromulina*$_{AND}$ and the original 1939 isolate of *Chrysochromulina parva* Lackey [29] are no longer in culture, thus genetic comparisons are not possible. Importantly, the presence of scales on several isolates identified as *Chrysochromulina parva* (Table 1, [29,38]) argues for a re-assignment of these scale-covered "*Chrysochromulina parva*" isolates to existing or new *Chrysochromulina* species.

2.5. Summary

- Morphological similarity is observed among freshwater *Chrysochromulina* isolates: The three scale-less, freshwater haptophyte isolates in this study maintain a very similar cellular profile, having a large nucleus nestled between two chloroplasts. Each chloroplast is associated with a prominent lipid body. A complex intracellular membrane system comprised of a network of tubular cristae, vesicles containing electron-opaque material, and a large wedge-shaped Golgi apparatus is evident. The flagellar apparatus, anchored in the cytoplasm by 4 microtubular roots, is composed of two flagellar bases and the haptonema, and interconnected by fibrous structures, some which are crossbanded.
- The diagnosis for the type species *Chrysochromulina parva* has been revisited: The freshwater unicell presently described in the literature as *Chrysochromulina parva* Lackey having a layer of scales on the cell surface and seven haptonemal microtubules in the emergent portion [29] is incorrect. Based on the observations presented here and molecular data [34], the diagnosis for the type species of *Chrysochromulina parva* needs to be emended to note that *Chrysochromulina parva* is a naked unicell having six microtubules present in the emergent part of the haptonema. Importantly, cultures or reports of scale-covered cells identified as *Chrysochromulina parva* need to be re-assigned as other or new *Chrysochromulina* species. Additionally, *Chrysochromulina*$_{AND}$ should be renamed when that organism has been re-isolated.
- Scale-less *Chrysochromulina* isolates comprise a cryptic species complex: Historically, morphological differences in scale architecture have been used to help define the boundaries of *Chrysochromulina* species. However, naked forms within this algal genus present a conundrum. These cosmopolitan and endemic cryptic morphotypes encompass an unexpected level of genetic diversity that has been only recently been explored [23,34]. Presently, by using molecular probes (e.g., 18S rDNA, *rbc*L), the distribution and phylogenetic richness of marine strains has been assessed, and the occurrence of freshwater strains analyzed [4]. Correlative morphological data is sorely absent.

3. Materials and methods

3.1. Algal source and culturing conditions

3.1.1.1 *Chrysochromulina tobinii* Cattolico (CCMP291) was acquired from NCMA by the Cattolico laboratory in 2006. This bacterized strain was designated as P3. Cells from the P3 cultures were subject to reiterative flow cytometry using BODIPY 505/515 (4,4-difluoro-1,3,5,7-tetramethyl-4-bora-3a,4a-diaza-s-indacene; Invitrogen, Carlsbad, CA) (see below for staining procedure) as the fluorophore for cell sorting purposes. Cells obtained from reiterative flow cytometric selection (P5.0) were treated in RAC-1 proprietary medium that contained either streptomycin (P5.5) or hygromycin (P5.6). Treatment for these two antibiotics were identical: cells were exposed to a final concentration of 400 μg/mL antibiotic for 18 h before 5 mL of treated cultures was transferred to 100 mL of RAC-1 medium lacking antibiotic. Cultures P5.5 and P5.6 were periodically tested for bacterial contamination using Luria-Bertani medium [71] made with RAC-1 medium. Determination of single bacterial contaminant was achieved by plating P5 cells on medium containing 0.1% glycerol. To test whether our P3 and P5 laboratory-maintained strains were genetically identical to the parent strain that had been maintained in the NCMA culture collection, *Chrysochromulina tobinii* Cattolico was re-ordered from NCMA in 2011 [10].

3.1.1.2 *Chrysochromulina parva* Lackey UW 1161 was isolated from water samples collected at Big Walnut Creek in Shadeville, OH (Latitude 39° 49′60" N; Longitude 82° 59′ 35" W), by Dr. Robert A. Andersen on September 24, 2014. This location was closest to that used to initially describe *Chrysochromulina parva* Lackey [26]. Water samples were overnight shipped to the University of Washington, filtered through 100 μm nylon mesh to minimize the presence of predatory organisms, and kept at 20 °C at 30 $\mu Em^{-2}s^{-1}$ in RAC-5 proprietary algal growth medium. In April 2015, once the culture was predominantly *Chrysochromulina parva*, fluorescence-activated cell sorting was performed at the Institute for Systems Biology to produce a unialgal

culture.

3.1.1.3 *Chrysochromulina*$_{AND}$ A2343 was collected in May 1981 by Celia Lopez from the Fox River near McHenry, Illinois (~ location 42.3234 N and 88.2523 W). The culture used in this study was initiated in March 1983 by Dr. Robert A. Andersen, maintained in a medium (2 L) that contained soil extract plus vitamins [https://ncma.bigelow.org/node/74], and fixed for transmission electron microscopy in April 1983. Though several EM blocks remain in our facility, the *Chrysochromulina*$_{AND}$ A2343 isolate is no longer available in culture.

3.1.1.4 All *Chrysochromulina* cultures were maintained in 250 mL Erlenmeyer flasks containing 100 mL of RAC-5 medium plugged with silicone sponge stoppers (Bellco Glass, Vineland, NJ) and capped with a sterilizer bag (Propper Manufacturing, Long Island City, NY). Larger volume experimental cultures were maintained in 1.0 L medium that was contained in a 2.8 L large-mouth Fernbach flask, plugged with hand-rolled, #50 cheese cloth-covered cotton stoppers, and covered with a #2 size Kraft bag (Paper Mart, Orange, CA). All cultures were maintained at 20 °C on a 12 h light:12 h dark photoperiod under 100 $\mu Em^{-2} s^{-1}$ light intensity using full spectrum T12 fluorescent light bulbs (Philips Electronics, Stamford, CT). No additional CO_2 was provided and cultures were not agitated. Cultures were sampled at hour ~6 in the light portion of the 12 h light:12 h dark photoperiod. Culture details for salinity tolerance experiments are presented in the Fig. 1S legend.

3.2. Electron microscopy

Chrysochromulina tobinii Cattolico or *Chrysochromulina parva* Lackey.

3.2.1. Scanning electron microscopy

Five hundred microliters of concentrated *Chrysochromulina tobinii* Cattolico or *Chrysochromulina parva* Lackey cell suspension was mixed with an equal volume of 2.0% glutaraldehyde in 0.2 M sodium cacodylate buffer (pH 7.2) at room temperature, then 250 µl of 4.0% osmium tetroxide was immediately added. The cells were fixed 15 min on ice, then filtered onto a 0.4 µm or 1 µm Nucleopore membrane (Nucleopore Corp., Pleasanton, CA), rinsed with 0.1 M sodium cacodylate buffer, then dehydrated to 100% alcohol (50%, 70%, 95%, 100%). Dehydrated cells on filters were critical point dried (Samdri 790 critical point dryer, Tousimis Research Corporation Rockville, MD), coated with 6 nm platinium (ES150T coater, Electron Microscopy Sciences, Hatfield, PA) and viewed in a Quanta 450 FESEM (FEI, Hillsboro, OR).

3.2.2. Transmission electron microscopy

Chrysochromulina tobinii Cattolico or *Chrysochromulina parva* Lackey cells were fixed using two different protocols which gave equivalent results. Cell pellets were fixed for 1 h in 2.0% glutaraldehyde in 0.15 M sodium cacodylate buffer (pH 7.2) at room temperature, then rinsed three times in buffer alone followed by 1.0% osmium tetroxide treatment in 0.15 M sodium cacodylate buffer (pH 7.2) for 1 h on ice. Alternatively, 1 mL of concentrated cell suspension was fixed with an equal volume of 4% glutaraldehyde in 0.15 M sodium cacodylate (pH 7.2) at room temperature, inverted to mix, then postfixed by the addition of 0.5 mL 4% osmium tetroxide for 15 min. Pellets of either fixation protocol were dehydrated in a graded alcohol series (50%, 70%, 95%, 100%), rinsed three times in 100% dry acetone, infiltrated in a graded acetone-EMBed812 series (33%, 66%, 100%), embedded in 100% EMBed812 (Electron Microscopy Sciences, Hatfield, PA), and polymerized at 60 °C. Silver sections were cut with a Diatome diamond knife (Electron Microscopy Sciences, Hatfield, PA), and viewed on a Tecnai 12 TEM (FEI, Hillsboro, OR) either unstained or stained with aqueous 2.0% uranyl acetate followed by lead citrate [72]. Images were recorded on an XR-41S 2k digital camera (Advanced Microscopy Techniques Corp., Woburn, MA).

3.2.3. Transmission electron microscopy for *Chrysochromulina*$_{AND}$

Four milliliters of concentrated *Chrysochromulina*$_{AND}$ A2343 cell culture was fixed with an equal volume of 4.0% glutaraldehyde made in 0.25 M sodium cacodylate buffer (pH 7.0) and mixed by inversion for 20 s, followed by the immediate addition of 2.0 mls 4.0% osmium tetroxide. These pellets were stained *en bloc* in aqueous 0.5% uranyl acetate, dehydrated in alcohol and embedded in Spurr's plastic. These EM blocks were maintained in storage at room temperature until 2013 when they were accessed for this study and examined as described above.

3.3. Cell staining

3.3.1. Mitochondrial

MitoTracker Green FM (Invitrogen, Eugene, OR) was resuspended in dimethyl sulfoxide (DMSO) to a final storage stock concentration of 1.0 mM, aliquoted and stored at −20 °C. The working stock solution of MitoTracker Green FM was prepared on the day of cell observation by adding 1 µL of 1.0 mM stock to 9.0 µL of RAC-1 algal growth medium. Early stationary phase *Chrysochromulina tobinii* Cattolico live cells were stained using 2.0 µL of working stock to 1.0 mL of cell culture, for a final dye concentration of 500 nM, and incubating in the dark at room temperature for at least 15 min. After incubation, 3.0 µL of methanol per 1.0 mL of cells was added to inhibit swimming for easier observation under the microscope. Mitochondria in approximately 40 individual cells were counted using a Zeiss Axioscop 2 Plus epifluorescent microscope equipped with a FITC filter.

3.3.2. Lipid body

A 5 mM BODIPY 505/515 (Invitrogen, Eugene, OR) working stock solution was prepared in 99% pure DMSO. This stock solution was added to live *Chrysochromulina tobinii* Cattolico cultures for a final BODIPY 505/515 concentration of 1–10 µM and gently mixed before being viewed on the fluorescent microscope [59].

3.4. Cell counts

Because of the minute size of *Chrysochromulina tobinii* Cattolico, special care was taken in assessing culture density by using a BD Accuri C6 flow cytometer (BD Biosciences, San Jose, CA). The *Chrysochromulina tobinii* Cattolico cells were counted and positively identified against background noise by exciting the samples with a 488 nm laser and detecting chlorophyll autofluorescence with the FL3 (670 nm LP) and FL4 (675/25 nm) channel detectors and then isolating the cellular chlorophyll signal from non-autofluorescent culture debris. Total overlap (by particle count) between gated cell populations and background was less than 1.0%. Expected count error was less than 1.0%.

3.5. DNA preparation, PCR, and sequencing

This is a brief summary of the methods used by Hovde et al. [34]. *Chrysochromulina tobinii* Cattolico and *Chrysochromulina parva* Lackey (UW 1161) cultures were grown in 1 L of RAC-5 medium until stationary phase, then 800 mL were centrifuged and stored at −80 °C. DNA was prepared using a modified Qiagen Genomic-tip protocol (Valencia, CA) [73]. A *Chrysochromulina parva* Lackey (NIES-562) cell pellet was obtained from NIES and DNA was prepared using the Qiagen Blood & Tissue kit. 18S rDNA PCR primers from Zhang et al. [74] and Thermo Scientific Hi-Fidelity Phusion DNA Polymerase (New England Biolabs, Ipswich, MA) were used with an annealing temperature of 68 °C for PCR. Sequencing reactions were performed using internal sequencing primers from Bendif [75], cleaned by ethanol precipitation, and sequenced on an ABI3130xl Sequencer (Life Technologies, Carlsbad, CA).

3.6. Phylogenetic inference

An 18S small ribosomal subunit phylogeny was generated using Bayesian Markov chain Monte Carlo and maximum likelihood methods. The data matrix included sequences for 21 *Chrysochromulina* terminal taxa and three outgroup haptophytes (*Emiliania huxleyi*, *Coccolithus pelagicus*, and *Cruciplaccolithus neohelis*). The sequence data consisted of 24 DNA sequences totaling 1785 aligned base pairs. Genes were aligned using MAFFT version 7.394 [76] with the X-INS-i strategy, which uses pairwise structural alignment for RNA sequences [77]. Bayesian analyses were implemented in MrBayes version 3.2.6 [78] and four independent Bayesian runs of four chains each (three heated chains with the heating parameter set to 0.20 and one cold chain) were run for 1×10^7 generations with a burn-in of 2.5×10^6 generations. Trees were sampled every 100 generations. The runs were considered to have adequately sampled the solution space when the standard deviation of split frequencies was below 5×10^{-3}. The same tree topology was independently constructed using maximum-likelihood (ML) methods implemented in RAxML version 8.2.10 [79]. The rapid bootstrap analysis was used and 850 ML replicate trees were used to estimate bootstrap support.

Competing interests

There are no competing interests associated with the publication of this manuscript.

Authors' contributions

RAC conceived, designed, and coordinated the study. SBB carried out all SEM and TEM morphological analysis. CRD and RAC generated the unialgal *Chrysochromulina parva* Lackey culture. CRD curated algal strains, isolated DNA, and performed PCR, sequencing, and analysis. BTH generated the phylogeny. All authors helped to draft the manuscript and read and approved the final product.

Acknowledgments

We wish to thank Dr. Robert A. Andersen (U. Washington) for providing an EM block for use in micro-anatomical analysis of *Chrysochromulina*$_{AND}$. Dr. Andersen also collected *Chrysochromulina parva* Lackey from the Big Walnut Creek, and gave editorial advice. Dr. Masanobu Kawachi (Center for Environmental and Ecosystem Studies, Japan) provided the *Chrysochromulina parva* NIES-562 cell pellet and DNA for PCR sequencing. Hannah Roberts (U. Washington) performed preliminary PCR for taxon identification of *Chrysochromulina tobinii* Cattolico, and Dr. Erik Hanschen (Los Alamos National Lab) helped generate the phylogeny. Dr. Bonnie Brewer (U. Washington) provided analysis of *Chysochromulina tobinii* Cattolico chromosome number. Dr. William Hardin (U. Washington) carried out preliminary physiology experiments and BODIPY 505/515 staining of *Chrysochromulina tobinii* Cattolico. RAC dedicates this manuscript to the global 'Me Too' movement.

Funding sources

Funding for BTH was provided by the Interdisciplinary Training in Genomic Sciences [NHGRI T32-HG00035] and an NSF Predoctoral Training Grant [DGE-0718124]. The authors acknowledge the use of equipment at the San Diego State University Electron Microscopy Facility acquired by NSF instrumentation grants [DBI-0959908] (SEM) and [DBI-030829] (TEM) to SBB. This research was funded by the US Department of Energy under contract [DE-EE0003046] awarded to the National Alliance for Advanced Biofuels and Bioproducts and NOAA [NA070AR4170007] to RAC.

Appendix A. Supplementary data

Supplementary data to this article can be found online at https://doi.org/10.1016/j.algal.2019.101492.

References

[1] L.K. Medlin, W.H.C.F. Kooistra, D. Potter, G.W. Saunders, R.A. Andersen, Phylogenetic relationships of the 'golden algae' (haptophytes, heterokont chromophytes) and their plastids, in: D. Bhattacharya (Ed.), Orig. Algae Their Plast, vol. 11, Springer, Vienna, 1997, pp. 187–219, , https://doi.org/10.1007/978-3-7091-6542-3_11.

[2] E.S. Egge, W. Eikrem, B. Edvardsen, Deep-branching novel lineages and high diversity of haptophytes in the Skagerrak (Norway) uncovered by 454 pyrosequencing, J. Eukaryot. Microbiol. 62 (2015) 121–140, https://doi.org/10.1111/jeu.12157.

[3] S. Theroux, Y. Huang, L. Amaral-Zettler, Comparative molecular microbial ecology of the spring haptophyte bloom in a greenland arctic oligosaline lake, Front. Microbiol. 3 (2012) 415, , https://doi.org/10.3389/fmicb.2012.00415.

[4] S. Gran-Stadniczeñko, L. Šupraha, E.D. Egge, B. Edvardsen, Haptophyte diversity and vertical distribution explored by 18S and 28S ribosomal RNA gene metabarcoding and scanning electron microscopy, J. Eukaryot. Microbiol. 64 (2017) 514–532, https://doi.org/10.1111/jeu.12388.

[5] M. Simon, P. López-García, D. Moreira, L. Jardillier, New haptophyte lineages and multiple independent colonizations of freshwater ecosystems, Environ. Microbiol. Rep. 5 (2013) 322–332, https://doi.org/10.1111/1758-2229.12023.

[6] J. Decelle, I. Probert, L. Bittner, Y. Desdevises, S. Colin, C. de Vargas, M. Galí, R. Simó, F. Not, An original mode of symbiosis in open ocean plankton, Proc. Natl. Acad. Sci. U. S. A. 109 (2012) 18000–18005, https://doi.org/10.1073/pnas.1212303109.

[7] B. Edvardsen, W. Eikrem, J. Throndsen, A.G. Sáez, I. Probert, L.K. Medlin, Ribosomal DNA phylogenies and a morphological revision provide the basis for a revised taxonomy of the Prymnesiales (Haptophyta), Eur. J. Phycol. 46 (2011) 202–228, https://doi.org/10.1080/09670262.2011.594095.

[8] M.L. Cuvelier, A.E. Allen, A. Monier, J.P. McCrow, M. Messié, S.G. Tringe, T. Woyke, R.M. Welsh, T. Ishoey, J.-H. Lee, B.J. Binder, C.L. DuPont, M. Latasa, C. Guigand, K.R. Buck, J. Hilton, M. Thiagarajan, E. Caler, B. Read, R.S. Lasken, F.P. Chavez, A.Z. Worden, Targeted metagenomics and ecology of globally important uncultured eukaryotic phytoplankton, Proc. Natl. Acad. Sci. U. S. A. 107 (2010) 14679–14684, https://doi.org/10.1073/pnas.1001665107.

[9] L. Bittner, A. Gobet, S. Audic, S. Romac, E.S. Egge, S. Santini, H. Ogata, I. Probert, B. Edvardsen, C. de Vargas, Diversity patterns of uncultured haptophytes unravelled by pyrosequencing in Naples Bay, Mol. Ecol. 22 (2013) 87–101, https://doi.org/10.1111/mec.12108.

[10] B.T. Hovde, C.R. Deodato, H.M. Hunsperger, S.A. Ryken, W. Yost, R.K. Jha, J. Patterson, R.J. Monnat, S.B. Barlow, S.R. Starkenburg, R.A. Cattolico, Genome sequence and transcriptome analyses of *Chrysochromulina tobin*: metabolic tools for enhanced algal fitness in the prominent order Prymnesiales (Haptophyceae), PLoS Genet. 11 (2015) e1005469, , https://doi.org/10.1371/journal.pgen.1005469.

[11] Z. Liu, A.E. Koid, R. Terrado, V. Campbell, D.A. Caron, K.B. Heidelberg, Changes in gene expression of *Prymnesium parvum* induced by nitrogen and phosphorus limitation, Front. Microbiol. 6 (2015) 631, , https://doi.org/10.3389/fmicb.2015.00631.

[12] A.R.J. Curson, B.T. Williams, B.J. Pinchbeck, L.P. Sims, A.B. Martínez, P.P.L. Rivera, D. Kumaresan, E. Mercadé, L.G. Spurgin, O. Carrión, S. Moxon, R.A. Cattolico, U. Kuzhiumparambil, P. Guagliardo, P.L. Clode, J.-B. Raina, J.D. Todd, DSYB catalyses the key step of dimethylsulfoniopropionate biosynthesis in many phytoplankton, Nat. Microbiol. 3 (2018) 430, https://doi.org/10.1038/s41564-018-0119-5.

[13] N. Bigelow, J. Barker, S. Ryken, J. Patterson, W. Hardin, S. Barlow, C. Deodato, R.A. Cattolico, *Chrysochromulina* sp.: a proposed lipid standard for the algal biofuel industry and its application to diverse taxa for screening lipid content, Algal Res. 2 (2013), https://doi.org/10.1016/j.algal.2013.07.001.

[14] M.-J. Chrétiennot-Dinet, N. Desreumaux, R. Vignes-Lebbe, An interactive key to the *Chrysochromulina* species (Haptophyta) described in the literature, PhytoKeys 34 (2014) 47–60, https://doi.org/10.3897/phytokeys.34.6242.

[15] K.H. Nicholls, Haptophyte algae, in: J. Wehr, R. Sheath, J.P. Kociolek (Eds.), Freshw. Algae North Am, 2nd ed., Elsevier, London, 2015, pp. 587–605, , https://doi.org/10.1016/B978-0-12-385876-4.00013-X.

[16] S. Seoane, W. Eikrem, R. Pienaar, B. Edvardsen, *Chrysochromulina palpebralis* sp. nov. (Prymnesiophyceae): a haptophyte, possessing two alternative morphologies, Phycologia 48 (2009) 165–176, https://doi.org/10.2216/08-63.1.

[17] V. Rousseau, F. Lantoine, F. Rodriguez, F. LeGall, M.-J. Chrétiennot-Dinet, C. Lancelot, Characterization of *Phaeocystis globosa* (Prymnesiophyceae), the blooming species in the Southern North Sea, J. Sea Res. 76 (2013) 105–113, https://doi.org/10.1016/J.SEARES.2012.07.011.

[18] M. Kawachi, I. Inouye, Functional roles of the haptonema and the spine scales in the feeding process of *Chrysochromulina spinifera* (Fournier) Pienaar et Norris (Haptophyta = Prymnesiophyta), Phycologia 34 (1995) 193–200, https://doi.org/10.2216/i0031-8884-34-3-193.1.

[19] R.W. Jordan, A.H.L. Chamberlain, Biodiversity among haptophyte algae, Biodivers. Conserv. 6 (1997) 131–152, https://doi.org/10.1023/A:1018383817777.

[20] B.S.C. Leadbetter, Cell Coverings, in: J.C. Green, B.S.C. Leadbetter (Eds.), The Haptophyte Algae, vol. 51, Clarendon Press, Oxford, 1994, pp. 23–46.

[21] E.M. Bendif, I. Probert, D.C. Schroeder, C. de Vargas, On the description of *Tisochrysis lutea* gen. nov. sp. nov. and I*sochrysis nuda* sp. nov. in the Isochrysidales, and the transfer of *Dicrateria* to the Prymnesiales (Haptophyta), J. Appl. Phycol. 25 (2013) 1763–1776, https://doi.org/10.1007/s10811-013-0037-0.

[22] K. Lekve, E. Bagøien, E. Dahl, B. Edvardsen, M. Skogen, N.C. Stenseth, Environmental forcing as a main determinant of bloom dynamics of the *Chrysochromulina* algae, Proc. Biol. Sci. 273 (2006) 3047–3055, https://doi.org/10.2307/25223720.

[23] H. Liu, I. Probert, J. Uitz, H. Claustre, S. Aris-Brosou, M. Frada, F. Not, C. de Vargas, Extreme diversity in noncalcifying haptophytes explains a major pigment paradox in open oceans, Proc. Natl. Acad. Sci. U. S. A. 106 (2009) 12803–12808, https://doi.org/10.1073/pnas.0905841106.

[24] C. Suttle, A. Chan, Viruses infecting the marine Prymnesiophyte *Chrysochromulina* spp.: isolation, preliminary characterization and natural abundance, Mar. Ecol. Prog. Ser. 118 (1995) 275–282, https://doi.org/10.3354/meps118275.

[25] K.H. Nicholls, Haptophyte algae, in: J.D. Wehr, R.G. Sheath (Eds.), Freshw. Algae North Am, Elsevier, San Diego, 2003, pp. 511–521, , https://doi.org/10.1016/B978-012741550-5/50014-3.

[26] J.B. Lackey, Notes on plankton flagellates from the Scioto River (with descriptions of new forms), Llyodia 2 (1939) 128–143.

[27] M. Parke, I. Manton, B. Clarke, Studies on marine flagellates II. Three new species of *Chrysochromulina*, J. Mar. Biol. Assoc. United Kingdom. 34 (1955) 579, https://doi.org/10.1017/S0025315400008833.

[28] M. Parke, I. Manton, B. Clarke, Studies on marine flagellates: III. Three further species of *Chrysochromulina*, J. Mar. Biol. Assoc. United Kingdom. 35 (1956) 387, https://doi.org/10.1017/S0025315400010225.

[29] M. Parke, J.W.G. Lund, I. Manton, Observations on the biology and fine structure of the type species of *Chrysochromulina* (*C. parva* Lackey) in the English Lake District, Arch. Mikrobiol. 42 (1962) 333–352, https://doi.org/10.1007/BF00409070.

[30] H.J. Kling, J. Kristiansen, Scale–bearing Chrysophyceae (Mallomonadaceae) from Central and Northern Canada, Nord. J. Bot. 3 (1983) 269–290, https://doi.org/10.1111/j.1756-1051.1983.tb01078.x.

[31] K.H. Nicholls, *Chrysochromulina breviturrita* sp. nov., a new freshwater member of the Prymnesiophyceae, J. Phycol. 14 (1978) 499–505, https://doi.org/10.1111/j.1529-8817.1978.tb02476.x.

[32] H.J. Kling, *Chrysochromulina laurentiana*: an electron microscopic study of a new species of Prymnesiophyceae from Canadian Shield lakes, Nord. J. Bot. 1 (1981) 551–555, https://doi.org/10.1111/j.1756-1051.1981.tb00722.x.

[33] D. Wujek, W. Gardiner, Chrysophyceae (Mallomonadaceae) from Florida. II. New species of *Paraphysomonas* and the prymnesiophyte *Chrysochromulina*, Florida Sci 48 (1985) 59–63.

[34] B. Hovde, C. Deodato, R. Andersen, S. Starkenburg, S. Barlow, R.A. Cattolico, *Chrysochromulina*: genomic assessment and taxonomic diagnosis of the type species for an oleaginous algal clade, Algal Res. 37 (2019) 307–319, https://doi.org/10.1016/j.algal.2018.11.023.

[35] S.F. Mirza, M.A. Staniewski, C.M. Short, A.M. Long, Y.V. Chaban, S.M. Short, Isolation and characterization of a virus infecting the freshwater algae *Chrysochromulina parva*, Virology 486 (2015) 105–115, https://doi.org/10.1016/j.virol.2015.09.005.

[36] R. Aguiar, Systematics and Ultrastructure of New and Rare Chrysophytes from Colorado and Wyoming Lakes, Ph.D. Dissertation Colorado State University, USA, 2000, https://doi.org/10.16953/deusbed.74839.

[37] M.M. Diaz, L.E. Lorenzo, *Chrysochromulina parva* Lackey (Prymnesiophyceae) new for South America, Algol. Stud. Für Hydrobiol. Suppl. (1990) 19–24 https://www.schweizerbart.de/papers/algol_stud/detail/60/66490/%23 , Accessed date: 9 March 2019.

[38] R.H. Thompson, P.J. Halicki, *Chrysochromulina parva* Lackey in Eastern Kansas, Trans. Am. Microsc. Soc. 84 (1965) 14, https://doi.org/10.2307/3224535.

[39] D. Wujek, L.C. Saha, *Chrysochromulina parva* Lackey (Prymnesiophyceae) a new record from India, Phykos 30 (1991) 169–171.

[40] L. Tauscher, Checklisten und Gefahrdungsgrade der Algen des Landes Brandenburg, Verh. Bot. Ver. Berlin Brand. 146 (2013) 109–128.

[41] W. Luo, C. Bock, H.R. Li, J. Padisák, L. Krienitz, Molecular and microscopic diversity of planktonic eukaryotes in the oligotrophic Lake Stechlin (Germany), Hydrobiologia 661 (2011) 133–143, https://doi.org/10.1007/s10750-010-0510-6.

[42] R. Ortiz-Álvarez, X. Triadó-Margarit, L. Camarero, E.O. Casamayor, J. Catalan, High planktonic diversity in mountain lakes contains similar contributions of autotrophic, heterotrophic and parasitic eukaryotic life forms, Sci. Rep. 8 (2018) 4457, , https://doi.org/10.1038/s41598-018-22835-3.

[43] Q.L. Wu, A. Chatzinotas, J. Wang, J. Boenigk, Genetic diversity of eukaryotic plankton assemblages in Eastern Tibetan Lakes differing by their salinity and altitude, Microb. Ecol. 58 (2009) 569–581, https://doi.org/10.1007/s00248-009-9526-8.

[44] M. Chen, F. Chen, B. Zhao, W. Qinglong L, F. Kong, Spatio-temporal variability of microbial eukaryotic community composition in a large shallow subtropical lake, assessed by 18S rRNA gene sequences, Acta Protozool. 48 (2009) 245–264.

[45] S. Charvet, W.F. Vincent, C. Lovejoy, Chrysophytes and other protists in High Arctic lakes: molecular gene surveys, pigment signatures and microscopy, Polar Biol. 35 (2012) 733–748, https://doi.org/10.1007/s00300-011-1118-7.

[46] L.M. Brown, R.J. Smith, R.R. Shivers, A.W. Day, A re-examination of the surface scales of *Chrysochromulina breviturrita* Nicholls (Prymnesiophyceae), Phycologia 25 (1986) 572–575.

[47] Z. Yi, C. Berney, H. Hartikainen, S. Mahamdallie, M. Gardner, J. Boenigk, T. Cavalier-Smith, D. Bass, High-throughput sequencing of microbial eukaryotes in Lake Baikal reveals ecologically differentiated communities and novel evolutionary radiations, FEMS Microbiol. Ecol. 93 (2017), https://doi.org/10.1093/femsec/fix073.

[48] M.Ø. Jensen, Ø. Moestrup, Ultrastructure of *Chrysochromulina ahrengotii* sp. nov. (Prymnesiophyceae), a new saddle-shaped species of *Chrysochromulina* from Danish coastal waters, Phycologia 38 (1999) 195–207, https://doi.org/10.2216/i0031-8884-38-3-195.1.

[49] W. Eikrem, Ø. Moestrup, Structural analysis of the flagellar apparatus and the scaly periplast in *Chrysochromulina scutellum* sp. nov. (Prymnesiophyceae, Haptophyta) from the Skagerrak and the Baltic, Phycologia 37 (1998) 132–153, https://doi.org/10.2216/i0031-8884-37-2-132.1.

[50] M. Birkhead, R.N. Pienaar, The flagellar apparatus of *Chrysochromulina* sp. (Prymnesiophyceae), J. Phycol. 31 (1995) 96–108, https://doi.org/10.1111/j.0022-3646.1995.00096.x.

[51] Ø. Moestrup, H.A. Thomsen, Ultrastructure and reconstruction of the flagellar apparatus in *Chrysochromulina apheles* sp. nov. (Prymnesiophyceae = Haptophyceae), Can. J. Bot. 64 (1986) 593–610, https://doi.org/10.1139/b86-077.

[52] J.D. Dodge, The Fine Structure of Algal Cells, Academic Press, New York, 1973.

[53] Y. Yoshida, S. Miyagishima, H. Kuroiwa, T. Kuroiwa, The plastid-dividing machinery: formation, constriction and fission, Curr. Opin. Plant Biol. 15 (2012) 714–721, https://doi.org/10.1016/j.pbi.2012.07.002.

[54] A.D. TerBush, Y. Yoshida, K.W. Osteryoung, FtsZ in chloroplast division: structure, function and evolution, Curr. Opin. Cell Biol. 25 (2013) 461–470, https://doi.org/10.1016/J.CEB.2013.04.006.

[55] S. Miyagishima, Y. Kabeya, Chloroplast division: squeezing the photosynthetic captive, Curr. Opin. Microbiol. 13 (2010) 738–746, https://doi.org/10.1016/J.MIB.2010.10.004.

[56] C. Magnussen, S.P. Gibbs, Behavior of chloroplast ER during chloroplast division in *Olisthodiscus luteus* (Chrysophyceae), J. Phycol. 16 (1980) 303–305, https://doi.org/10.1111/j.1529-8817.1980.tb03035.x.

[57] T. Fujimoto, Y. Ohsaki, J. Cheng, M. Suzuki, Y. Shinohara, Lipid droplets: a classic organelle with new outfits, Histochem. Cell Biol. 130 (2008) 263–279, https://doi.org/10.1007/s00418-008-0449-0.

[58] L. Yang, Y. Ding, Y. Chen, S. Zhang, C. Huo, Y. Wang, J. Yu, P. Zhang, H. Na, H. Zhang, Y. Ma, P. Liu, The proteomics of lipid droplets: structure, dynamics, and functions of the organelle conserved from bacteria to humans, J. Lipid Res. 53 (2012) 1245–1253, https://doi.org/10.1194/jlr.R024117.

[59] M.S. Cooper, W.R. Hardin, T.W. Petersen, R.A. Cattolico, Visualizing “green oil” in live algal cells, J. Biosci. Bioeng. 109 (2010) 198–201, https://doi.org/10.1016/j.jbiosc.2009.08.004.

[60] N.W. Bigelow, W.R. Hardin, J.P. Barker, S.A. Ryken, A.C. MacRae, R.A. Cattolico, A comprehensive GC–MS sub-microscale assay for fatty acids and its applications, J. Am. Oil Chem. Soc. 88 (2011) 1329–1338, https://doi.org/10.1007/s11746-011-1799-7.

[61] I. Manton, Further observations on the microanatomy of the haptonema in *Chrysochromulina chiton* and *Prymnesium parvum*, Protoplasma 66 (1968) 35–53, https://doi.org/10.1007/BF01252523.

[62] D.J. Hibberd, Prymnesiophytes (=Haptophytes), in: E.R. Cox (Ed.), Dev. Mar. Biol, vol. 2, Elsevier North Holland, New York, 1980, pp. 273–317.

[63] A.J. Gregson, J.C. Green, B.S.C. Leadbeater, Structure and physiology of the haptonema in *Chrysochromulina* (Prymnesiophyceae). I. Fine structure of the flagellar/haptonematal root system in *C. acantha* and *C. simplex*, J. Phycol. 29 (1993) 674–686, https://doi.org/10.1111/j.0022-3646.1993.00674.x.

[64] A.J. Gregson, J.C. Green, B.S.C. Leadbeater, Structure and physiology of the haptonema in *Chrysochromulina* (Prymnesiophyceae). II. Mechanisms of haptonematal coiling and the regeneration process, J. Phycol. 29 (1993) 686–700, https://doi.org/10.1111/j.0022-3646.1993.00686.x.

[65] K. Estep, F. Maclntyre, Taxonomy, life cycle, distribution and dasmotrophy of *Chrysochromulina*: a theory accounting for scales, haptonema, muciferous bodies and toxicity, Mar. Ecol. Prog. Ser. 57 (1989) 11–21, https://doi.org/10.3354/meps057011.

[66] Alga-Gro Concentrated Medium (Carolina Biological, Burlington, NC), (n.d.). https://www.carolina.com/biological-media-ingredients/alga-gro-concentrated-medium/FAM_153751.pr.

[67] B. Edvardsen, Life cycle strategies in the haptophyte genera *Chrysochromulina* and *Prymnesium*, in: E. Garces, A. Zingone, M. Montresor, B. Reguera, B. Dale (Eds.), Lifehab Life Hist. Microalgal Species Causing Harmful Bloom, 12th ed., 2002, pp. 67–70 Calvia.

[68] K.J. Niklas, E.D. Cobb, U. Kutschera, Did meiosis evolve before sex and the evolution of eukaryotic life cycles? BioEssays 36 (2014) 1091–1101, https://doi.org/10.1002/bies.201400045.

[69] K. Shalchian-Tabrizi, K. Reier-Roberg, D.K. Ree, D. Klaveness, J. Brate, Marine-freshwater colonizations of haptophytes inferred from phylogeny of environmental 18S rDNA sequences, J. Eukaryot. Microbiol. 58 (2011) 315–318, https://doi.org/10.1111/j.1550-7408.2011.00547.x.

[70] A. Saez, G. Probert, P. Quinn, J. Young, L. Medlin, Pseudo-cryptic speciation in coccolithophores, PNAS 100 (2003) 7163–7168, https://doi.org/10.1073/pnas.1132069100.

[71] G. Bertani, Studies on lysogenesis. I. The mode of phage liberation by lysogenic *Escherichia coli*, J. Bacteriol. 62 (1951) 293–300.

[72] E.S. Reynolds, The use of lead citrate at high pH as an electron-opaque stain in electron microscopy, J. Cell Biol. 17 (1963) 208–212, https://doi.org/10.1083/JCB.17.1.208.

[73] R.A. Cattolico, M.A. Jacobs, Y. Zhou, J. Chang, M. Duplessis, T. Lybrand, J. McKay, H.C. Ong, E. Sims, G. Rocap, Chloroplast genome sequencing analysis of *Heterosigma akashiwo* CCMP452 (West Atlantic) and NIES293 (West Pacific) strains, BMC Genomics 9 (2008) 211, https://doi.org/10.1186/1471-2164-9-211.

[74] H. Zhang, D. Bhattacharya, S. Lin, Phylogeny of dinoflagellates based on

mitochondrial cytochrome b and nuclear small subunit rDNA sequence comparisons, J. Phycol. 41 (2005) 411–420, https://doi.org/10.1111/j.1529-8817.2005.04168.x.

[75] E.M. Bendif, I. Probert, A. Hervé, C. Billard, D. Goux, C. Lelong, J.-P. Cadoret, B. Véron, Integrative taxonomy of the Pavlovophyceae (Haptophyta): a reassessment, Protist 162 (2011) 738–761, https://doi.org/10.1016/J.PROTIS.2011.05.001.

[76] K. Katoh, D.M. Standley, MAFFT multiple sequence alignment software version 7: improvements in performance and usability, Mol. Biol. Evol. 30 (2013) 772–780, https://doi.org/10.1093/molbev/mst010.

[77] K. Katoh, H. Toh, Improved accuracy of multiple ncRNA alignment by incorporating structural information into a MAFFT-based framework, BMC Bioinformatics 9 (2008) 212, , https://doi.org/10.1186/1471-2105-9-212.

[78] F. Ronquist, M. Teslenko, P. Van Der Mark, D.L. Ayres, A. Darling, S. Höhna, B. Larget, L. Liu, M.A. Suchard, J.P. Huelsenbeck, MrBayes 3.2: efficient bayesian phylogenetic inference and model choice across a large model space, Syst. Biol. 61 (2012) 539–542, https://doi.org/10.1093/sysbio/sys029.

[79] A. Stamatakis, RAxML version 8: a tool for phylogenetic analysis and post-analysis of large phylogenies, Bioinformatics 30 (2014) 1312–1313, https://doi.org/10.1093/bioinformatics/btu033.